Re-entry into quiescence protects hematopoietic stem cells from the killing effect of chronic exposure to type I interferons

Eric M. Pietras, Ranjani Lakshminarasimhan, Jose-Marc Techner, Sarah Fong, Johanna Flach, Mikhail Binnewies, and Emmanuelle Passegué

The Eli and Edythe Broad Center for Regenerative Medicine and Stem Cell Research, Department of Medicine, Division of Hematology/Oncology, University of California San Francisco, San Francisco, California 94143

Type I interferons (IFN-1s) are antiviral cytokines that suppress blood production while paradoxically inducing hematopoietic stem cell (HSC) proliferation. Here, we clarify the relationship between the proliferative and suppressive effects of IFN-1s on HSC function during acute and chronic IFN-1 exposure. We show that IFN-1–driven HSC proliferation is a transient event resulting from a brief relaxation of quiescence-enforcing mechanisms in response to acute IFN-1 exposure, which occurs exclusively in vivo. We find that this proliferative burst fails to exhaust the HSC pool, which rapidly returns to quiescence in response to chronic IFN-1 exposure. Moreover, we demonstrate that IFN-1–exposed HSCs with reestablished quiescence are largely protected from the killing effects of IFNs unless forced back into the cell cycle due to culture, transplantation, or myeloablative treatment, at which point they activate a p53-dependent proapoptotic gene program. Collectively, our results demonstrate that quiescence acts as a safeguard mechanism to ensure survival of the HSC pool during chronic IFN-1 exposure. We show that IFN-1s can poise HSCs for apoptosis but induce direct cell killing only upon active proliferation, thereby establishing a mechanism for the suppressive effects of IFN-1s on HSC function.

CORRESPONDENCE
Emmanuelle Passegué:
passeguee@stemcell.ucsf.edu

Abbreviations used: 5-FU, 5-fluorouracil; CC3, cleaved caspase-3; CDK, cyclin-dependent kinase; CKI, cyclin kinase inhibitor; CML, chronic myelogenous leukemia; CMP, common myeloid progenitor; EdU, 5-ethynyl-2'-deoxyuridine; ET, essential thrombocytopenia; GMP, granulocyte-macrophage progenitor; Gr, granulocyte; HSC, hematopoietic stem cell; IFNAR, type-I IFN receptor; LSC, leukemic stem cell; LSK, Lineage$^-$/c-Kit$^+$/Sca-1$^+$; MEP, megakaryocyte-erythrocyte progenitor; MP, myeloid progenitor; MPN, myeloproliferative neoplasm; MPP, multipotent progenitor; poly I:C, poly inosinic:cytidylic acid; PV, polycythemia vera; SLE, systemic lupus erythematosis; TKI, tyrosine kinase inhibitor.

Type I IFNs (IFN-1s) are a family of over 13 cytokines that interfere with viral replication via activation of their surface receptor, IFNAR, and subsequent receptor-dependent phosphorylation of the transcription factors STAT-1 and STAT-2 (Platanias, 2005). IFN-1s mediate host immune responses to viruses and intracellular pathogens, and drive autoimmune diseases such as systemic lupus erythematosus (SLE; Platanias, 2005; Davis et al., 2011). Moreover, IFN-1s have been used therapeutically to treat several diseases, including viral infections and myeloid malignancies such as chronic myelogenous leukemia (CML; Kiladjian et al., 2011).

Although the role of IFN-1s in immune cell biology is well studied, investigations into the effects of IFN-1s on blood-forming hematopoietic stem cells (HSCs) have only recently begun. HSCs are a rare population of immature self-renewing BM cells that produce all the lineages of blood cells, including those comprising the immune system, by differentiating through a series of progenitor cells (Orkin and Zon, 2008). Under homeostatic conditions, HSCs are primarily kept in the quiescent, or G_0, phase of the cell cycle as a means of limiting the potential for damage associated with cellular activation (Bakker and Passegué, 2013). Quiescence is enforced via the concerted activity of several mechanisms, including high expression of cyclin kinase inhibitors (CKIs) and transcriptional regulators such as FoxO3a and p53, as well as activation of extrinsic pathways, such as TGF-β, and Notch signaling (Pietras et al., 2011). However, HSCs can rapidly enter the cell cycle and proliferate in response to blood loss, activating cytokines or hematopoietic injury such as treatment with a myeloablative agent (Wilson et al., 2008). Paradoxically, although IFN-1s can

The Rockefeller University Press $30.00
J. Exp. Med. 2014 Vol. 211 No. 2 245-262
www.jem.org/cgi/doi/10.1084/jem.20131043

The Journal of Experimental Medicine

induce cell cycle arrest in hematopoietic progenitors (Verma et al., 2002), HSCs from mice treated with purified IFN-1s or the IFN-1 inducer polyinosinic:polycytidylic acid (poly I:C) rapidly enter the cell cycle in a manner requiring direct IFNAR signaling and activation of STAT-1 and AKT (Essers et al., 2009). Moreover, mice deficient in the transcription factor *Irf2*, the mRNA editing enzyme *Adar1* or the p47-family GTPase *Irgm1* exhibit IFN-dependent hyper-proliferation and loss of HSC numbers (Feng et al., 2008; Sato et al., 2009; Hartner et al., 2009). In addition, chronic administration of poly I:C leads to selective depletion of normal HSCs in WT:*Ifnar1*$^{-/-}$ BM chimeric mice, presumably due to proliferation-induced loss of wild-type HSCs (Essers et al., 2009). Collectively, these results suggest that, despite their known antiproliferative effects, IFN-1s activate HSC cell cycle activity in vivo and deplete HSCs due to a phenomenon known as proliferation-associated functional exhaustion (Orford and Scadden, 2008).

Many human patients treated with IFN-1s, as well as individuals suffering from IFN-associated chronic disease, exhibit profound hematologic effects, including sustained cytopenias, anemia, and thrombocytopenias (Gokce et al., 2012). However, chronic IFN exposure rarely causes BM failure in the absence of complicating factors (Zhou et al., 2007; Ioannou et al., 2010). Furthermore, the rate of complete cytogenetic response in CML patients treated with IFN-1s has been low (Talpaz et al., 1991), suggesting that IFN-1s alone are marginally effective in eliminating quiescent leukemic HSCs that give rise to the disease. These clinical results indicate that while chronic IFNs suppress blood production, they likely do not exhaust the HSC pool. In addition, the relationship between IFN-induced HSC proliferation and suppression of HSC function, particularly in the context of chronic IFN-1 exposure where the proliferative status of HSCs has not been directly assessed, remains unclear (Passegué and Ernst, 2009).

In the present study, we use a comprehensive battery of in vivo and in vitro approaches to clarify the relationship between the proliferative and suppressive effects of IFN-1s on HSC function during both acute and chronic IFN-1 exposure. We find that acute IFN-1 exposure induces transient HSC proliferation in vivo as the consequence of a brief decrease in expression of several key quiescence-enforcing mechanisms. This proliferative burst, and its associated molecular features, is not recapitulated in vitro, where IFN-1s exert a direct antiproliferative effect on cultured HSCs without affecting such quiescence-enforcing mechanisms. Importantly, the transient in vivo pro-proliferative activity of acute IFN-1 treatment fails to exhaust the HSC pool, which subsequently returns to a quiescent state during chronic IFN-1 exposure. Moreover, these quiescent IFN-1–exposed HSCs are largely protected from the killing effects of chronic IFN-1s unless they are forced back into the cell cycle by ex vivo culture, transplantation, or recovery after myeloablation treatment, at which point they activate a p53-dependent proapoptotic gene program resulting in cell death. These findings demonstrate that IFN-1–exposed HSCs are primed for apoptosis but are not killed until they are required to proliferate. Collectively, they provide critical new insights into how IFN-1s regulate HSC function, which have significant implications for our understanding of the relationship between inflammation, autoimmunity, and HSC biology.

RESULTS

Chronic IFN-1 exposure causes BM aplasia

To understand how acute and chronic IFN-1 exposure affects hematopoiesis, we analyzed the changes occurring in the BM of WT mice injected with poly I:C every second day over a time course ranging from 1 d (1 injection) to 30 d (15 injections; Fig. 1 A). We confirmed surface expression of the IFNAR1 receptor subunit on all mature and immature BM compartments (not depicted), and IFN-1 production in the sera of poly I:C–treated mice (Fig. 1 A). After an acute spike of IFN-1s produced by the first poly I:C injection, we measured low but detectable chronic production of IFN-1s from 3 to 30 d of continuous poly I:C treatment. In response to IFN-1 production, we observed a rapid and sustained IFNAR-dependent depletion of BM cells, corresponding to a decrease in mature Gr-1$^+$/Mac-1$^+$ granulocytes (Gr) and B220$^+$ B lymphocytes (B; Fig. 1, B and C; and Fig. S1 A). This BM cell depletion was associated with a widespread and sustained IFNAR-dependent apoptosis in the BM cavity as measured by immunofluorescence staining for cleaved caspase-3 (CC3; Fig. 1 D). We also found an IFNAR-dependent increase in serum levels of proinflammatory cytokines, including TNF and the IFN-inducible chemokine MCP-1 in poly I:C–treated mice (Fig. 1 E). These systemic changes were associated with a rapid decrease in lymphoid cells in the blood and peritoneal cavity, and a late increase in Gr in the spleen and peritoneal cavity (Fig. 1 F), which together argue against a major mobilizing effect, at least during the first 2 wk of poly I:C treatment. Collectively, these results demonstrate that 30 d of continuous poly I:C treatment results in a sustained BM aplastic phenotype in the context of elevated BM apoptosis and chronic systemic inflammation, similar to what is observed in human patients with chronic IFN-1 production (Gokce et al., 2012). We therefore consider 1–3 d of poly I:C treatment to represent acute IFN-1 exposure, and 5–30 d of continuous poly I:C treatment to accurately mimic chronic IFN-1 exposure.

Chronic IFN-1 exposure does not exhaust the HSC pool

We then addressed how chronic IFN-1 exposure affects the number of HSCs and other early progenitor cells in the BM. Similar to a previous study using IFN-γ (Zhao et al., 2009), we observed a significant expansion in the frequency of Lin$^-$/c-Kit$^+$/Sca1$^+$ (LSK) cells in poly I:C–treated mice, which normally consists of Flk2$^+$ LSK multipotent progenitors (MPP^{F+}), Flk2$^-$/CD48$^+$ LSK MPPs (MPP^{F-}), and Flk2$^-$/CD48$^-$/CD150$^+$ LSK HSCs (Fig. 2 A and Fig. S1 B). This increase mainly reflected an elevated frequency of MPP^{F-} in the LSK compartment of poly I:C–treated mice, and was accompanied by a substantial decrease in the frequency of

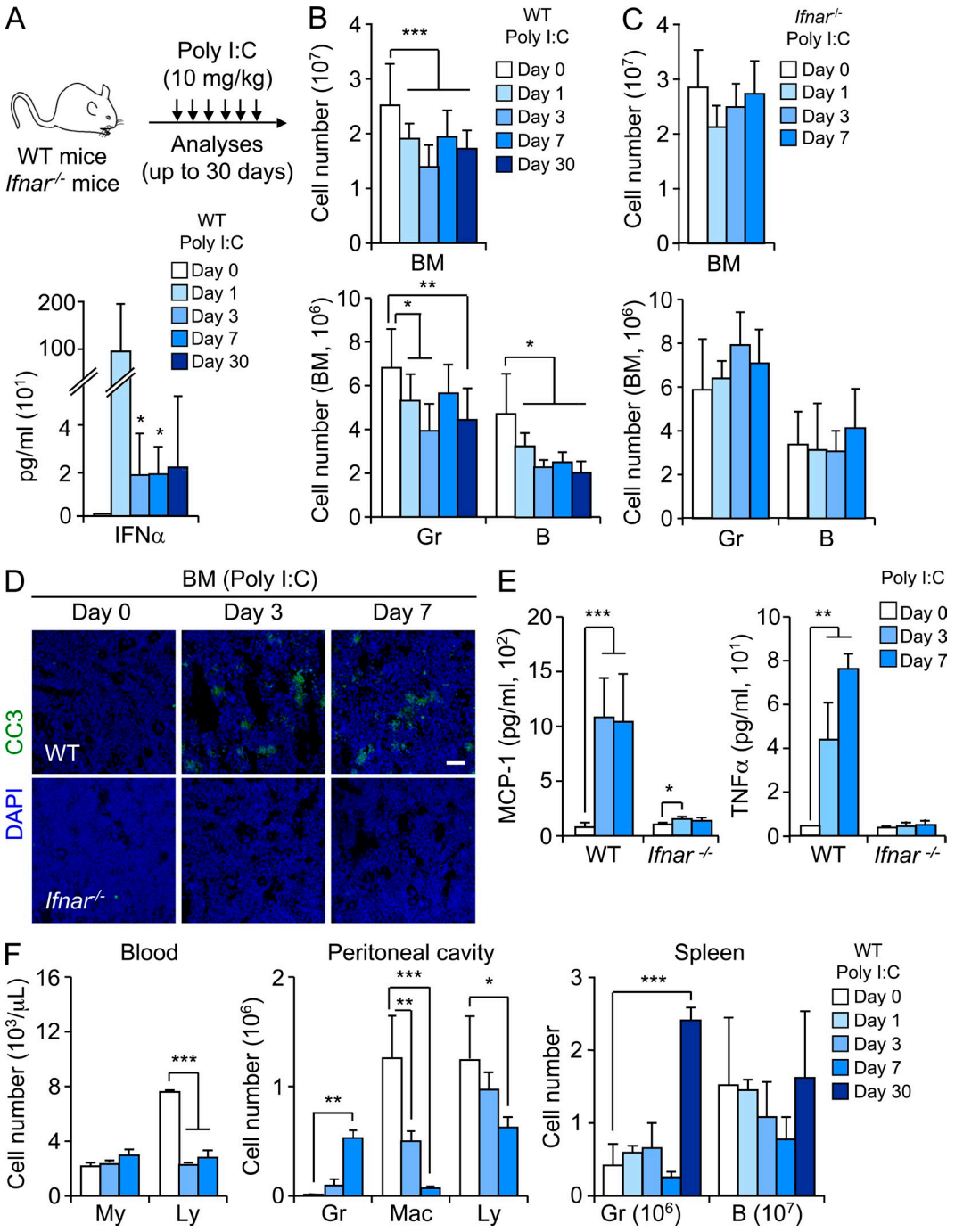

Figure 1. Chronic IFN-1 exposure induces BM aplasia. (A) Experimental design for acute and chronic poly I:C treatment in mice (top) and serum IFN-α levels in poly I:C–treated WT mice (bottom; 3–9 mice/group). (B) Mean BM cellularity and numbers of granulocytes (Gr) and B cells (B) in one femur and one tibia of poly I:C–treated mice (6–22 mice/group). (C) Mean BM cellularity and numbers of Gr and B cells in one femur and one tibia of poly I:C–treated *Ifnar1*$^{-/-}$ mice (4–5 mice/group). (D) Immunofluorescence imaging of cleaved caspase-3 (CC3) in femur sections of poly I:C–treated WT and *Ifnar*$^{-/-}$ mice. Bar, 50 µm. (E) MCP-1 and TNF serum levels in poly I:C–treated WT and *Ifnar1*$^{-/-}$ mice (3–8 mice/group). (F) Mean myeloid (My) and lymphoid (Ly) cell numbers in peripheral blood (left; 3–5 mice/group); granulocyte (Gr), macrophage (Mac), and lymphocyte (Ly) cell numbers in peritoneal cavity (center; 3–6 mice/group); Gr and B cell numbers in spleens (right; 3–12 mice/group) of poly I:C–treated mice. All data are mean ± SD; statistical significance was determined by Student's *t*-test (*, $P \leq 0.05$; **, $P \leq 0.01$; ***, $P \leq 0.005$).

$CD34^+/FcγR^-/Lin^-/c\text{-}Kit^+/Sca1^-$ common myeloid progenitors (CMP) in the $Lin^-/c\text{-}Kit^+/Sca1^-$ myeloid progenitor (MP) compartment (Fig. 2 A). These changes were entirely dependent on IFNAR signaling and not observed in the BM of poly I:C–injected *Ifnar1*$^{-/-}$ mice (Fig. 2 B). As a consequence of this increase in MPP^{F-} frequency, the percentage

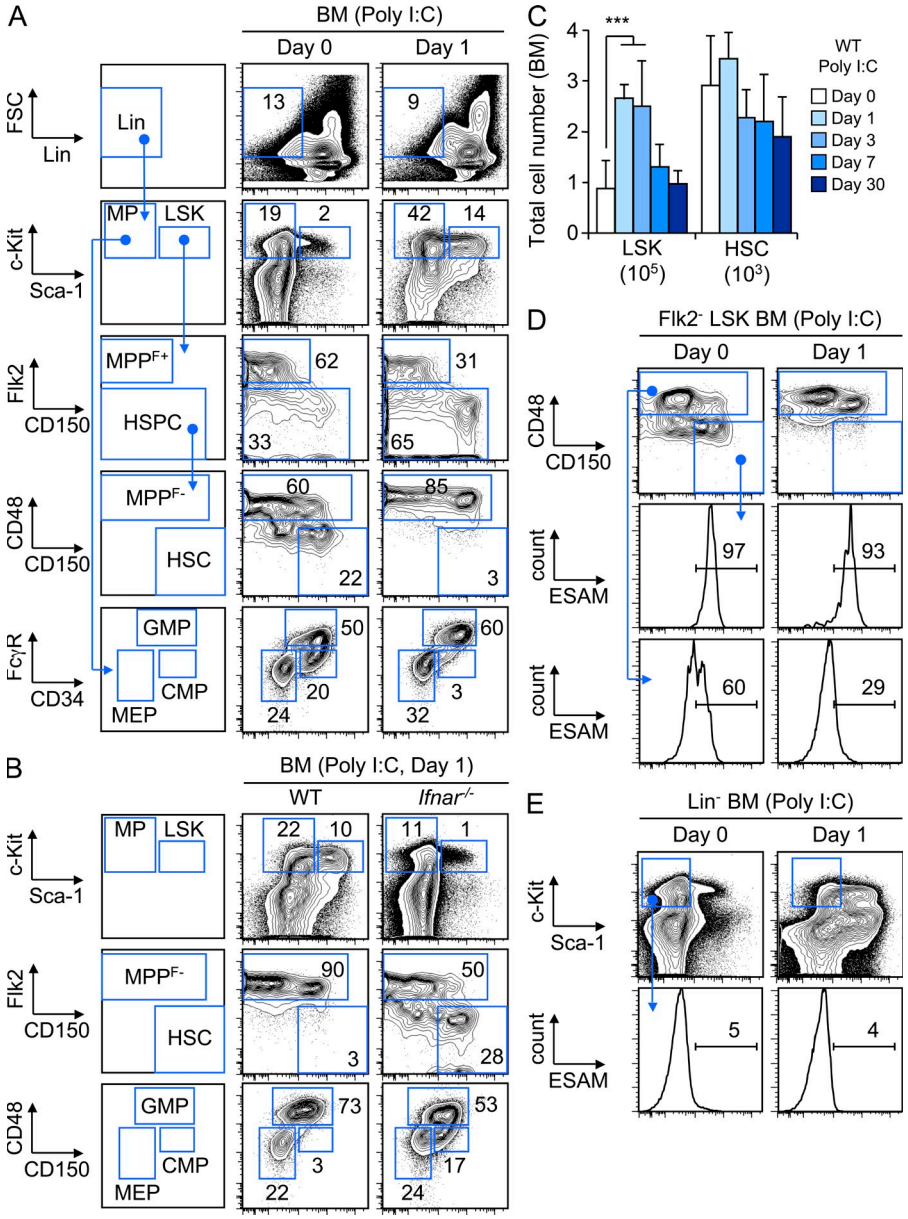

Figure 2. Chronic IFN-1 exposure does not alter the size of the HSC compartment. (A) Representative FACS plots for immature stem and progenitor cell populations in the BM of control and 1-d poly I:C–treated mice. (B) Representative FACS plots of stem and progenitor cells in the BM of 1-d poly I:C–treated WT and *Ifnar1*$^{-/-}$ mice. (C) Mean numbers of LSK and HSCs in one femur and tibia of poly I:C–treated mice (6–22 mice/group). (D and E) Representative FACS plots for ESAM expression in the Flk2^{-} LSK (D) and myeloid progenitor (E) compartments of control and 1-d poly I:C–treated mice. ***, $P \leq 0.005$.

of HSCs in the LSK compartment of poly I:C–treated mice also decreased over time (Fig. S1 B). However, when the mean cell number for each of these populations was calculated based on their frequency in the BM and the actual BM cellularity at each time point, we found a significant increase in LSK number, whereas the total number of HSCs remained essentially unchanged in poly I:C–treated mice even after 30 d of continuous treatment (Fig. 2 C).

Because IFN-1s are well-known inducers of Sca-1 expression (Dumont and Coker, 1986) resulting in increased Sca-1 levels over the poly I:C treatment period (Fig. S1 B), we directly investigated the purity of the HSC compartments using the HSC-specific marker ESAM (Ooi et al., 2009). As in untreated HSCs, we found that the vast majority of IFN-1–exposed HSCs were ESAM^{+} (Fig. 2 D), hence confirming their positive identification and lack of contamination by ESAM^{-} MPs (Fig. 2 E). In contrast, we observed an increased proportion of ESAM^{-} MPs in the phenotypic MPP^{F-} gate (Fig. 2 D). To gain further insights into the identity of these contaminating cells, we directly treated naive HSCs and early progenitors with IFN-α (100 ng/ml) for 12 h in vitro (Fig. 3 A). As expected, IFN-1s increased Sca-1 expression on already Sca-1–expressing HSCs, MPP^{F+} and MPP^{F-} (Fig. 3 B), but also reactivated Sca-1 expression on initially Sca-1 negative myeloid progenitors CMPs, GMPs, and MEPs (Fig. 3 C). In line with our in vivo data, contaminating progenitor cells that have regained or augmented Sca-1 expression only increased the frequency of MPP^{F-}, but not the frequency of HSCs, within the LSK gate (Fig. 3, B and C). Importantly, no other surface markers defining HSC identity were affected by addition

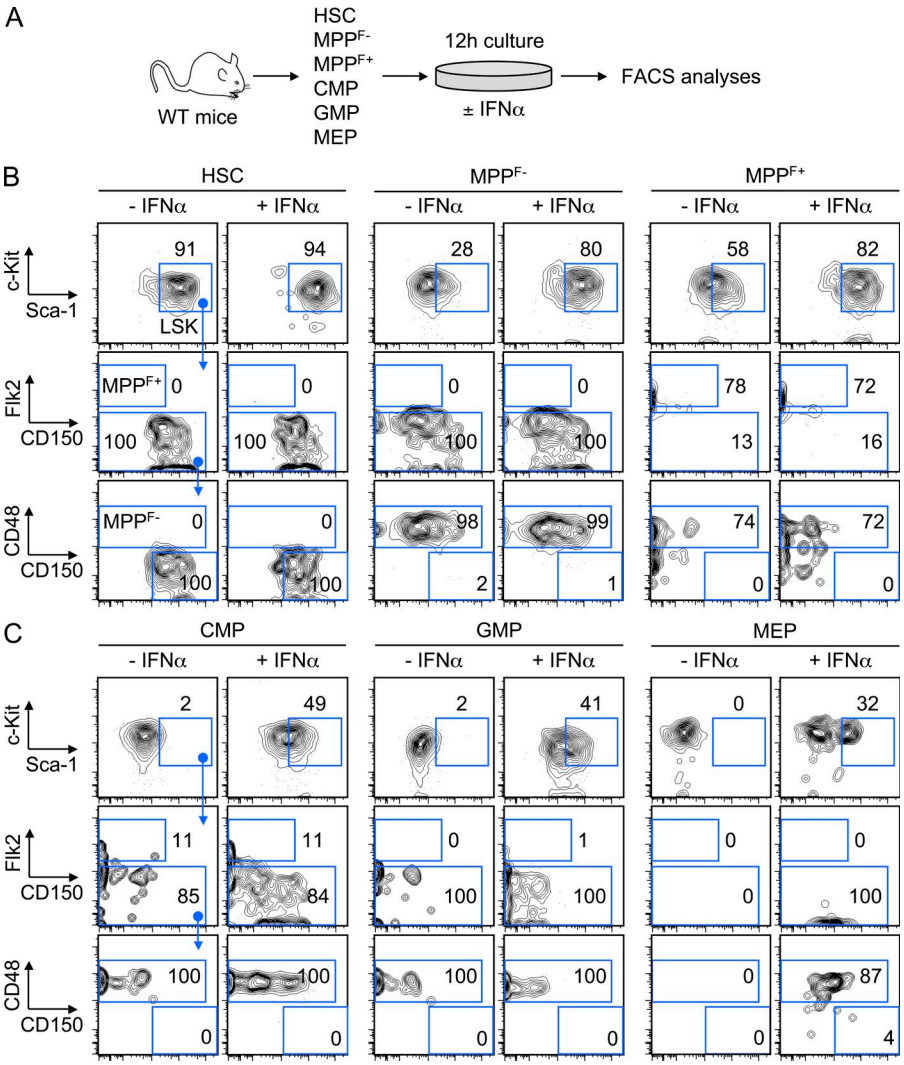

Figure 3. IFN-1 exposure reactivates Sca-1 expression in myeloid progenitors. (A) Experimental design for FACS analysis of naive hematopoietic populations cultured for 12 h ± 100 ng/ml IFN-α. (B and C) Representative FACS plots and frequency of HSC surface markers on Sca-1–expressing LSK populations (B) and Sca-1$^-$ myeloid progenitors (C) cultured for 12 h ± 100 ng/ml IFN-α.

of IFN-α, and none of the IFN-1–treated progenitors acquired a Flk2$^-$/CD48$^-$/CD150$^+$ HSC surface phenotype. These results indicate that the phenotypic distinction between MPs and MPPs becomes blurred upon IFN-1 exposure, and that the LSK expansion in poly I:C–treated mice is mainly the result of contaminating MPs that have reacquired Sca-1 expression. They also show that the Flk2$^-$/CD48$^-$/CD150$^+$ HSC compartment remains free of contaminating progenitor cells even in conditions of IFN-1–driven Sca-1 expression. Collectively, these data indicate that IFN-1s induce a rapid phenotypic BM remodeling, particularly in the LSK compartment, but do not deplete HSCs.

Rapid but transient increase in HSC proliferation during chronic IFN-1 exposure

Acute IFN-1 exposure rapidly induces HSC proliferation (Essers et al., 2009), but whether HSCs continue to cycle in the presence of chronic IFN-1s is unknown. To investigate how IFN-1s affect HSC cell cycle activity over time, we injected 5-bromodeoxyuridine (BrdU) 3 h before sacrificing poly I:C–treated mice and measured BrdU incorporation in HSCs (Fig. 4 A and Fig. S2 A). Consistent with prior results (Essers et al., 2009), we found that IFN-1s rapidly induced HSC proliferation by 12 h, with BrdU incorporation peaking after 1–3 d of poly I:C treatment. However, HSC BrdU incorporation rapidly returned to basal levels by 5 d of poly I:C treatment, and then largely remained steady even after 30 d of continuous poly I:C administration (Fig. 4 B). We then characterized the cell cycle distribution of HSCs during this period using intracellular Ki67/DAPI FACS staining (Fig. S2 B). In agreement with the BrdU results, we observed a significant decrease in quiescent (G_0) HSCs by 3 d of poly I:C treatment, with a corresponding increase in the proportion of HSCs in G_1 and S-G_2/M phases of the cell cycle (Fig. 4 C). However, the HSC compartment returned to a predominantly quiescent phenotype by 7 d of poly I:C treatment, though this quiescent phenotype appeared to gradually erode over prolonged IFN-1 exposure. We also observed a similar transient

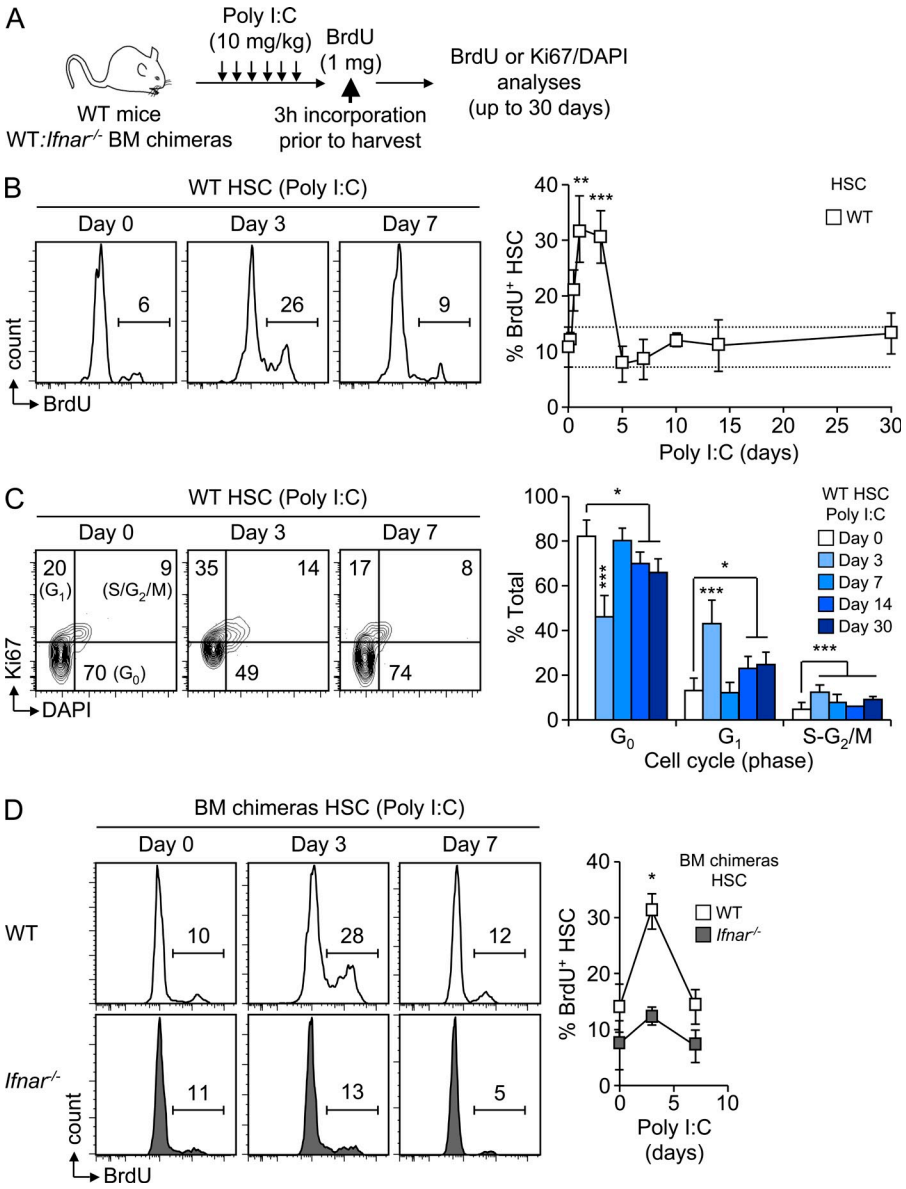

Figure 4. Chronic IFN-1 exposure transiently increases HSC proliferation.
(A) Experimental design for HSC cell cycle analyses in poly I:C–treated WT and WT:*Ifnar1*$^{-/-}$ chimeric mice. (B) Representative FACS plots (left) and mean levels (right) of HSC BrdU incorporation (3–13 mice/group). (C) Representative FACS plots (left) and mean HSC distribution (right) in cell cycle phases (3–13 mice/group). (D) Representative FACS plots (left) and mean levels (right) of BrdU incorporation in WT (CD45.1^{+}) and *Ifnar1*$^{-/-}$ (CD45.2^{+}) HSCs from WT:*Ifnar1*$^{-/-}$ BM chimeric mice (3–4 mice/group). All data are mean ± SD; statistical significance was determined by Student's *t*-test (*, $P \leq 0.05$; **, $P \leq 0.01$; ***, $P \leq 0.005$).

increase in HSC proliferation in WT mice injected with 1×10^4 units of mouse recombinant IFN-α every 12 h for up to 7 d, with increased BrdU incorporation by day 1 and a return to steady-state levels by day 7 (unpublished data). This indicates that the short HSC cycling response is not restricted to poly I:C treatment or is the direct consequence of the spike in IFN-1 production after the initial poly I:C injection (Fig. 1 B). We also generated WT:*Ifnar1*$^{-/-}$ BM chimeric mice to directly test the involvement of IFNAR signaling. We confirmed the 50:50 distribution of WT:*Ifnar1*$^{-/-}$ cells in the blood and HSC compartment 2 mo after transplantation (unpublished data), and used BrdU incorporation to analyze the proliferation of WT and *Ifnar1*$^{-/-}$ HSCs side-by-side in the same chimeric animal after poly I:C injection (Fig. 4 D). Notably, WT but not *Ifnar1*$^{-/-}$ HSCs proliferated for a brief period of time, thus demonstrating that the transient IFN-mediated HSC proliferation is a direct consequence of IFNAR signaling. Collectively, these results indicate that IFN-1 exposure induces a rapid but transient, rather than sustained, proliferation in HSCs, which quickly return to a quiescent state during chronic exposure.

IFN-1s transiently antagonize expression of HSC quiescence-enforcing mechanisms in vivo

We then investigated how chronic IFN-1s could induce transient HSC proliferation in vivo. We first assessed the status of the AKT/PKB–FoxO3a pathway, which is directly activated by IFN-1 (Yamazaki et al., 2006; Essers et al., 2009) and is essential to regulate the switch between quiescence and proliferation in HSCs (Pietras et al., 2011), by measuring AKT phosphorylation levels in HSCs using intracellular FACS staining (Fig. S2 C). Interestingly, we found that the kinetics

of AKT phosphorylation mirrored those of HSC proliferation, with a peak in phosphorylation at day 3, followed by a return to basal phospho-AKT levels by day 7 of poly I:C treatment (Fig. 5 A). Furthermore, the quiescence-enforcing transcription factor FoxO3a was predominantly sequestered in the cytoplasm and therefore inactivated at day 3 when HSCs were cycling, and relocalized in the nucleus at day 7 when HSCs had relapsed into quiescence (Fig. 5 B). We then used a custom-made SA Biosciences PCR array to assess expression of cell cycle genes and key genes associated with

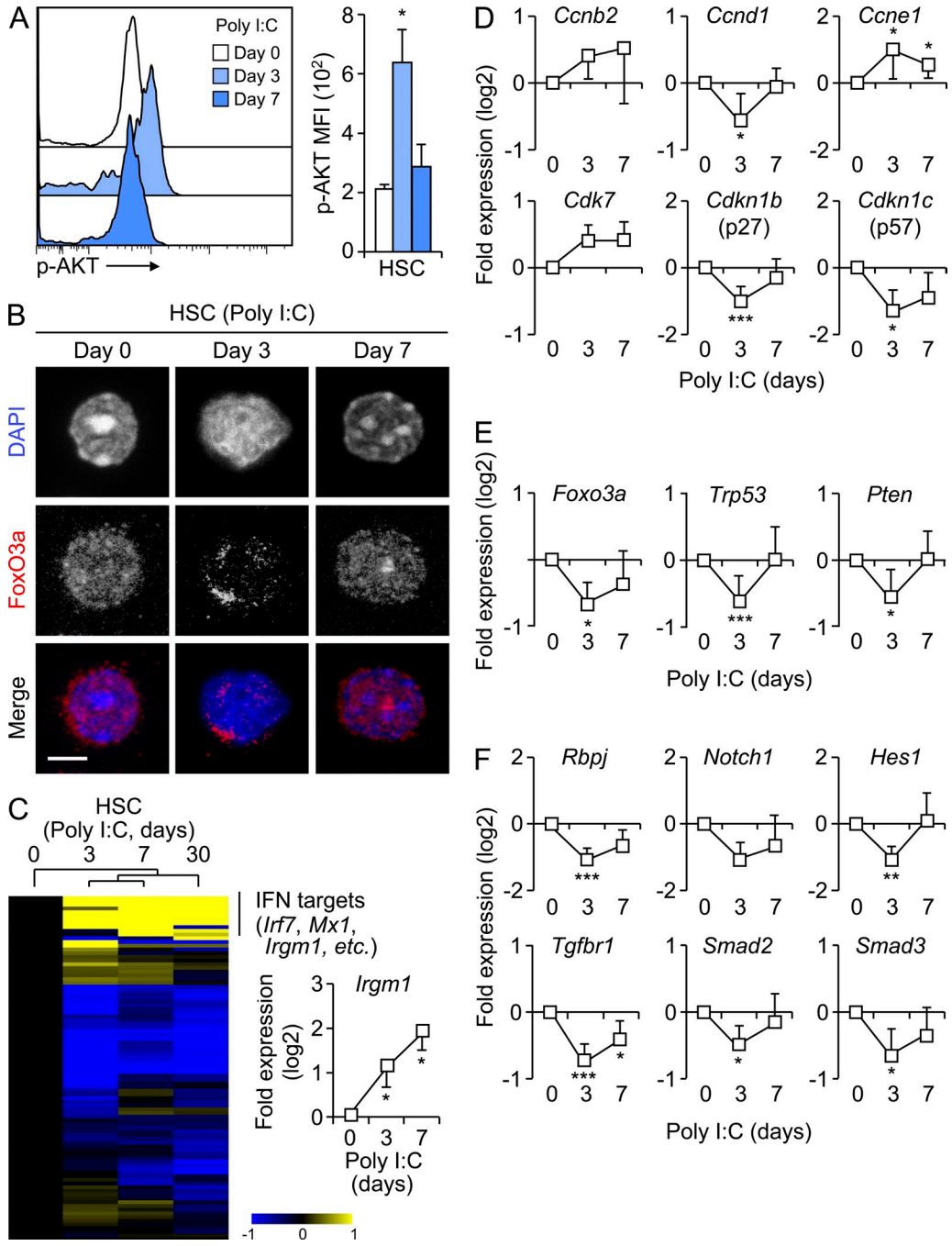

Figure 5. IFN-1s transiently antagonize expression of HSC quiescence-enforcing mechanisms in vivo. (A) Representative histograms (left) and average mean fluorescence intensity (MFI, right) for phospho-AKT (p-AKT) levels in CD48⁻ LSK HSCs from poly I:C–treated mice (3 mice/group). (B) Representative immunofluorescence staining of FoxO3a localization in HSCs from poly I:C–treated mice. Bar, 5 µm. (C–F) SABiosciences PCR array analyses of HSCs from poly I:C–treated mice (n = 4, pools of 5 mice/group). (C) Hierarchical clustering of gene expression data (left) and *Irgm1* expression (right). (D) Expression of cell cycle and (E and F) quiescence-enforcing machinery genes. Results are expressed as $\log_2$ fold relative to day 0 controls. All data are mean ± SD; statistical significance was determined by Student's *t* test (*, $P \leq 0.05$; ***, $P \leq 0.005$).

quiescence-enforcing programs in HSCs at days 0, 3, 7, and 30 of poly I:C treatment (Fig. 5 C). We confirmed induction of IFN-1 target genes by poly I:C treatment at all time points, while expression of IFNAR1 and other IFN signaling pathway components did not decrease (Fig. 5 C and not depicted), indicating that HSCs were capable of responding to IFN-1s throughout the time course. Notably, expression of *Irgm1*, a negative regulator of IFN-mediated HSC cell cycle activity (King et al., 2011), was maximal in day 7 when HSCs had reentered quiescence (Fig. 5 C). However, except for IFN-1 targets, we observed a broad transcriptional repression throughout the treatment time course, which was noticeably more accentuated in cycling day 3 HSCs. In particular, we did not find substantial induction of cyclin and cyclin-dependent kinase (CDK) genes that drive HSC proliferation other than a transient increase in *Ccne1* (cyclin E1) expression in cycling day 3 HSCs (Fig. 5 D). Instead, we found significantly decreased expression of many quiescence-enforcing genes, including the cyclin-dependent kinase inhibitors (CKI) *Cdkn1b* (*p27*) and *Cdkn1c* (*p57*), the transcription factors *Foxo1*, *Foxo3a*, and *Trp53,* and the AKT inhibitor *Pten* in cycling day 3 HSCs, which subsequently returned to steady-state levels at day 7 when HSCs had relapsed into quiescence (Fig. 5 E and not depicted). Moreover, we observed a similar trend in two other quiescence-enforcing signaling mechanisms, with a transient decrease in expression of TGF-β and Notch pathway components and targets in cycling day 3 HSCs and restoration in day 7 HSCs that have reentered quiescence (Fig. 5 F). Collectively, these results demonstrate that cell cycle machinery is not directly activated by IFN-1s in vivo and, instead, that multiple quiescence-enforcing mechanisms are transiently antagonized and subsequently reactivated during chronic IFN-1 exposure.

Direct IFN-1 signaling does not induce HSC proliferation in vitro

We next tested whether IFN-1s could also exert a proproliferative effect in vitro by culturing purified HSCs in the presence of increasing concentrations of IFN-α. We found that addition of IFN-α did not enhance HSC proliferation in vitro, and directly antagonized HSC growth at a 100 ng/ml concentration, a dose previously shown to induce HSC proliferation in vitro in IFN-γ (Baldridge et al., 2010; Fig. 6 A). We confirmed this result using methylcellulose cultures of purified HSCs, where treatment with 100 ng/ml IFN-α significantly decreased cloning efficiency and colony size (Fig. 6 B). We next measured BrdU incorporation after 12 h of culture with or without 100 ng/ml IFN-α (Fig. 6 C), and found no increase in HSC proliferation upon direct IFN-1 stimulation. To test whether signals from other BM cells are required to induce HSCs to proliferate in response to IFN-1 in vivo, we co-cultured purified and CFSE-labeled WT or IFNAR-deficient HSCs with unfractionated WT BM cells in the presence or absence of IFN-α, and analyzed BrdU incorporation by flow cytometry during the culture period (Fig. 6 D and Fig. S3 A). However, even in this co-culture system, IFN-α did not enhance HSC proliferation or cell division at low concentrations and remained antiproliferative at higher concentrations (Fig. 6 D and not depicted). This inhibitory effect required IFNAR expression on HSCs, as BrdU incorporation by co-cultured *Ifnar1*$^{-/-}$ HSCs/BM cells was unaffected by IFN-α compared with WT HSCs/BM cells (Fig. 6 D). Moreover, co-culture of WT HSCs with BM cells from 1-d poly I:C–treated mice also reduced HSC proliferation (unpublished data). To further try and recapitulate the conditions in the BM niche, we co-cultured purified Violet-dye–labeled HSCs on OP9-DL1 stromal cells in the presence or absence of IFN-α and analyzed EdU incorporation during the 12-h culture period by immunofluorescence (Fig. 6 E and Fig. S3 B). However, even in these conditions, IFN-α inhibited HSC proliferation in vitro. This antiproliferative effect appeared to be a property common to all IFNs, as HSC proliferation after 12 h of culture with 100 ng/ml IFN-γ was also inhibited (unpublished data). We then investigated the expression of cell cycle genes and key genes associated with quiescence-enforcing programs in HSCs cultured for 12 h in the presence or absence of IFN-α (Fig. 6 F). As expected, we found no evidence of activated cell cycle machinery in HSCs cultured with IFN-α, but also did not observe the relaxation of quiescence-enforcing mechanisms occurring in day 3 cycling HSCs in vivo. Instead, we found significantly decreased levels of *Ccnd1* (*Cyclin D1*) and increased expression of *Cdkn1b* (*p27*) and *Cdkn1c* (*p57*), similar to in HSCs cultured with IFN-γ (de Bruin et al., 2013). Together, these results demonstrate that direct IFN-1 stimulation, regardless of the concentration, fails to induce HSC proliferation in vitro. This reinforces our finding that the transient proliferative effect observed in vivo likely results from a relaxation of multiple HSC quiescence-enforcing mechanisms rather than a direct activation of the cell cycle machinery.

Reacquisition of quiescence in IFN-exposed HSCs fails to restore HSC function

Because loss of function has been associated with HSC proliferation induced by IFNs (Essers et al., 2009; King et al., 2011), we investigated whether the reacquisition of quiescence in chronic IFN-1–exposed HSCs confers functional protection. We used HSCs isolated from mice treated with poly I:C for either 3 (cycling) or 7 (quiescent) days to assess their short-term potential in vitro and long-term potential in vivo (Fig. 7 A). Strikingly, both colony formation in methylcellulose and expansion rates in liquid culture were severely impaired in IFN-1–exposed HSCs regardless of the duration of poly I:C treatment and HSC cell cycle status at the time of harvest (Fig. 7 B). Consistent with these in vitro results, we found similarly decreased engraftment in recipient mice transplanted with IFN-exposed day 3 (cycling) or day 7 (quiescent) HSCs (Fig. 7 C). We confirmed that defective reconstitution was not the result of changes in lineage distribution (not depicted), but was caused by reduced BM chimerism and the number of engrafted donor-derived IFN-1–exposed HSCs (Fig. 7, D and E). Moreover, we found similar functional

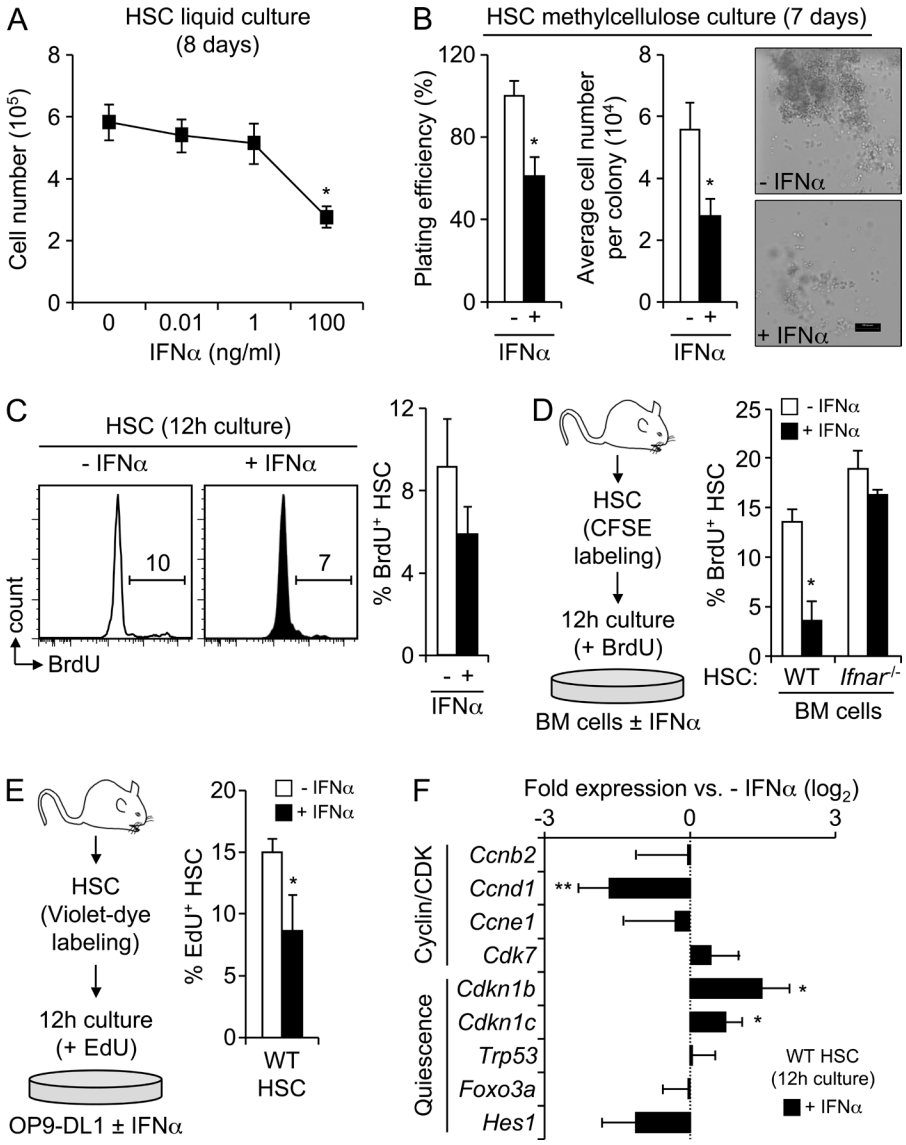

Figure 6. Direct IFN-1 signaling does not induce HSC proliferation in vitro. (A) Mean expansion rate of HSCs grown in the presence of the indicated concentrations of IFN-α in one representative experiment performed in triplicate. (B) Mean number (left), size (center), and pictograms (right; bar, 100 µm) of HSC-derived colonies grown in methylcellulose ± 100 ng/ml IFN-α in one representative experiment performed in triplicate. (C) Representative FACS plots (left) and mean levels (right) of BrdU incorporation in HSCs cultured for 12 h ± 100 ng/ml IFN-α ($n = 3$). (D) Experimental design (left) and mean levels (right) of BrdU incorporation in CFSE-labeled WT or *Ifnar1*$^{-/-}$ HSCs after 12 h co-culture with WT BM cells ± 100 ng/ml IFN-α ($n = 3$). (E) Experimental design (left) and mean levels (right) of EdU incorporation in Violet-labeled HSCs after 12-h co-culture with OP9-DL1 cells ± 100 ng/ml IFN-α ($n = 3$). (F) Quantitative RT-PCR analysis for expression of cell cycle and quiescence-enforcing genes in HSCs cultured for 12 h ± 100 ng/ml IFN-α ($n = 3$–4). Results are expressed as $\log_2$ fold relative to IFN-α controls. All data are mean ± SD; statistical significance was determined by Student's *t* test (*, $P \leq 0.05$; **, $P \leq 0.01$).

impairments in HSCs isolated from mice treated for 30 d with poly I:C (unpublished data). Collectively, these data indicate that chronic IFN-1 treatment impairs HSC function regardless of the length of exposure and its transient effect on HSC proliferation in vivo.

IFN-1 exposure kills HSCs upon cell cycle entry

We next assessed whether the loss of function observed in IFN-1–exposed HSCs could be caused by induction of apoptosis. IFN-1s have been shown to be proapoptotic in numerous cell types, including hematopoietic cells (Kiladjian et al., 2011), but their effect on HSC survival has never been directly tested. We first measured apoptosis levels in HSCs isolated from mice treated with poly I:C for either 3 or 7 d, and analyzed either directly upon harvest or after 12 h in vitro culture to force quiescent HSCs to proliferate (Fig. 8 A). When assayed directly upon isolation, we only observed increased CC3 activity in cycling day 3 HSCs, in contrast to quiescent day 7 HSCs (Fig. 8 B). However, upon culture, both day 3 and 7 HSCs exhibited a significant and IFNAR-dependent increase in CC3 activity (Fig. 8 C). Consistently, we also found elevated CC3 levels in HSCs isolated from day 7 IFN-α–injected mice after 12-h in vitro culture (Fig. 8 D). These proapoptotic effects were reversible, as a 2-wk recovery period after 7 d of poly I:C treatment in vivo (day 7 + 2 wk) largely restored HSC survival and function in methylcellulose cultures and upon transplantation (Fig. 8, E and F). To gain molecular insights, we then used our SA Biosciences PCR array and direct qRT-PCR analyses to investigate the status of the apoptotic machinery and expression of *Bcl2* family members in IFN-1–exposed HSCs. Strikingly, we did not observe increased expression of any of the proapoptotic genes in freshly isolated day 3 HSCs (Fig. 8 G). Instead, we found a significant decrease in the expression of the essential prosurvival gene *Mcl1* in cycling day 3 HSCs, which likely contributes to their decreased survival compared with quiescent day 7 HSCs.

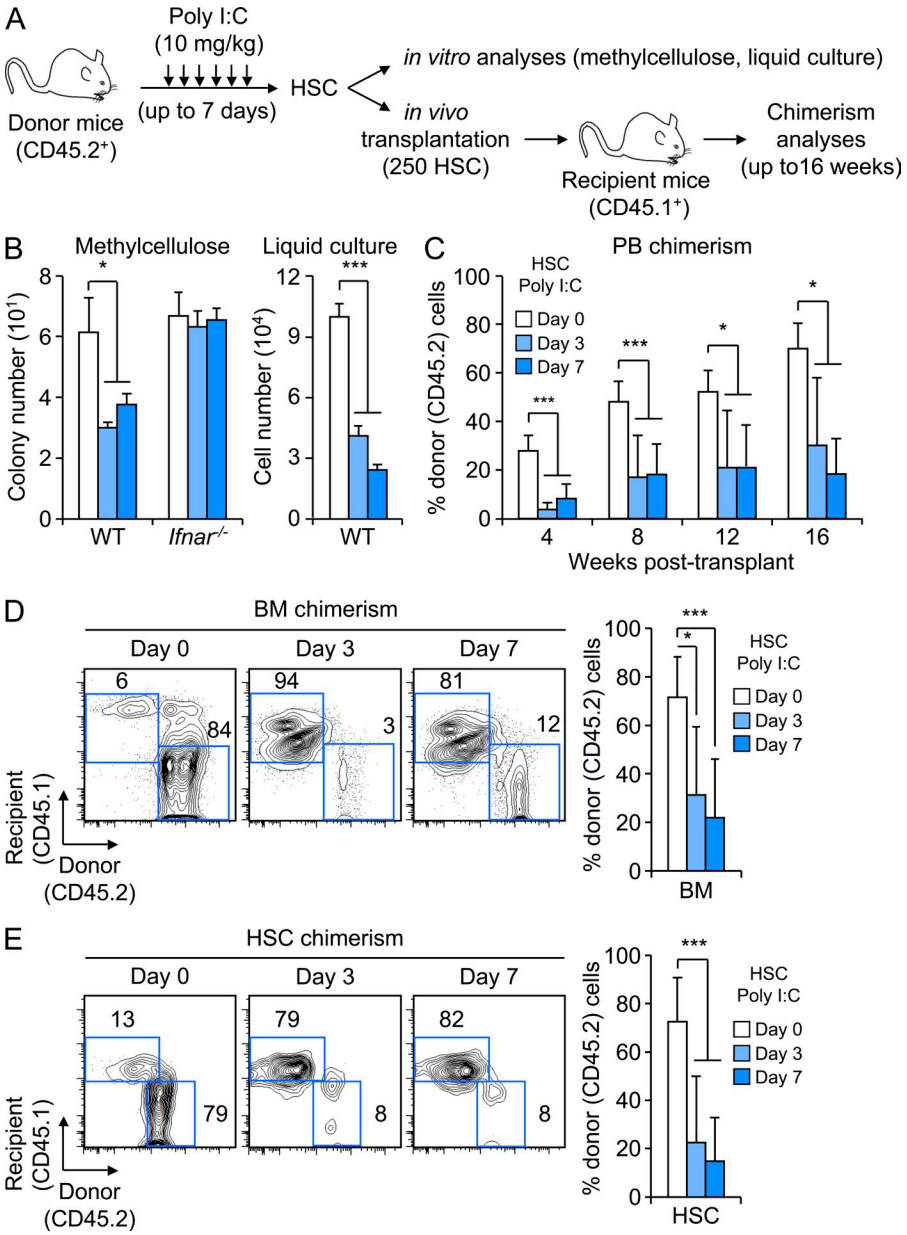

Figure 7. Reacquisition of quiescence fails to provide functional protection to IFN-exposed HSCs. (A) Experimental design for HSC functional testing. (B) Mean number of colonies in 7-d methylcellulose culture (left) and cells in 8-d liquid culture (right) obtained with HSCs isolated from poly I:C–treated WT and *Ifnar1*$^{-/-}$ mice in one representative experiment performed in triplicate. (C–E) Lethally irradiated recipient mice (CD45.1^{+}, 6 mice/group) were transplanted with 250 HSCs isolated from poly I:C–treated WT donor mice (CD45.2^{+}; pools of 3 mice/group). (C) PB chimerism over 16 wk after transplantation. (D) Representative FACS plots (left) and mean percentage (right) of donor-derived CD45.2^{+} BM cells in 16 wk post-transplantation mice. (E) Representative FACS plots (left) and mean percentage (right) of donor-derived CD45.2^{+} BM HSCs in 16 wk post-transplantation mice. All data are mean ± SD; statistical significance was determined by Student's *t* test (*, P ≤ 0.05; ***, P ≤ 0.005).

In sharp contrast, day 7 HSCs cultured for 12 h showed a rapid and significant increase in expression of proapoptotic *Bax*, *Puma*, and *Noxa* genes (Fig. 8 H). Collectively, these results indicate that IFN-1 exposure, regardless of its duration, poises HSCs for apoptosis but only results in direct cell killing in proliferating HSCs either due to a reduction in prosurvival factors in cells with transiently antagonized quiescence-enforcing mechanisms, or to activation of a pro-apoptotic gene program in cells that are actively forced to enter the cell cycle.

Function of p53 in IFN-1–exposed HSCs

IFN-1s are known to regulate the proapoptotic machinery via activation of p53 (Takaoka, et al., 2003). To probe the role of p53 in mediating the effects of IFN-1s on HSCs, we treated HSCs isolated from control (Ctrl) or *Trp53*$^{-/-}$ mice with IFN-α for 12 h in vitro (Fig. 9 A). Although IFN-α exposure induced CC3 activity and triggered *Bax*, *Puma*, and *Noxa* expression in control HSCs (Fig. 9, B and C), no CC3 induction and significantly decreased activation of the proapoptotic genes was found in IFN-α–treated *Trp53*$^{-/-}$ HSCs (Fig. 9, B and D). Moreover, no CC3 induction was observed in *Bak-Bax*-deficient HSCs upon treatment with IFN-α for 12 h in vitro (Fig. 9 B), thus validating the role of the intrinsic mitochondrial apoptotic pathway in the proapoptotic effects of IFN-1s on HSCs. Because p53 is also a critical enforcer of HSC quiescence (Pietras et al., 2011), we next investigated its importance for the in vivo proproliferative effect of IFN-1s on HSCs by measuring BrdU incorporation in poly I:C–treated control or *Trp53*$^{-/-}$ mice (Fig. 9 E). However, IFN-1

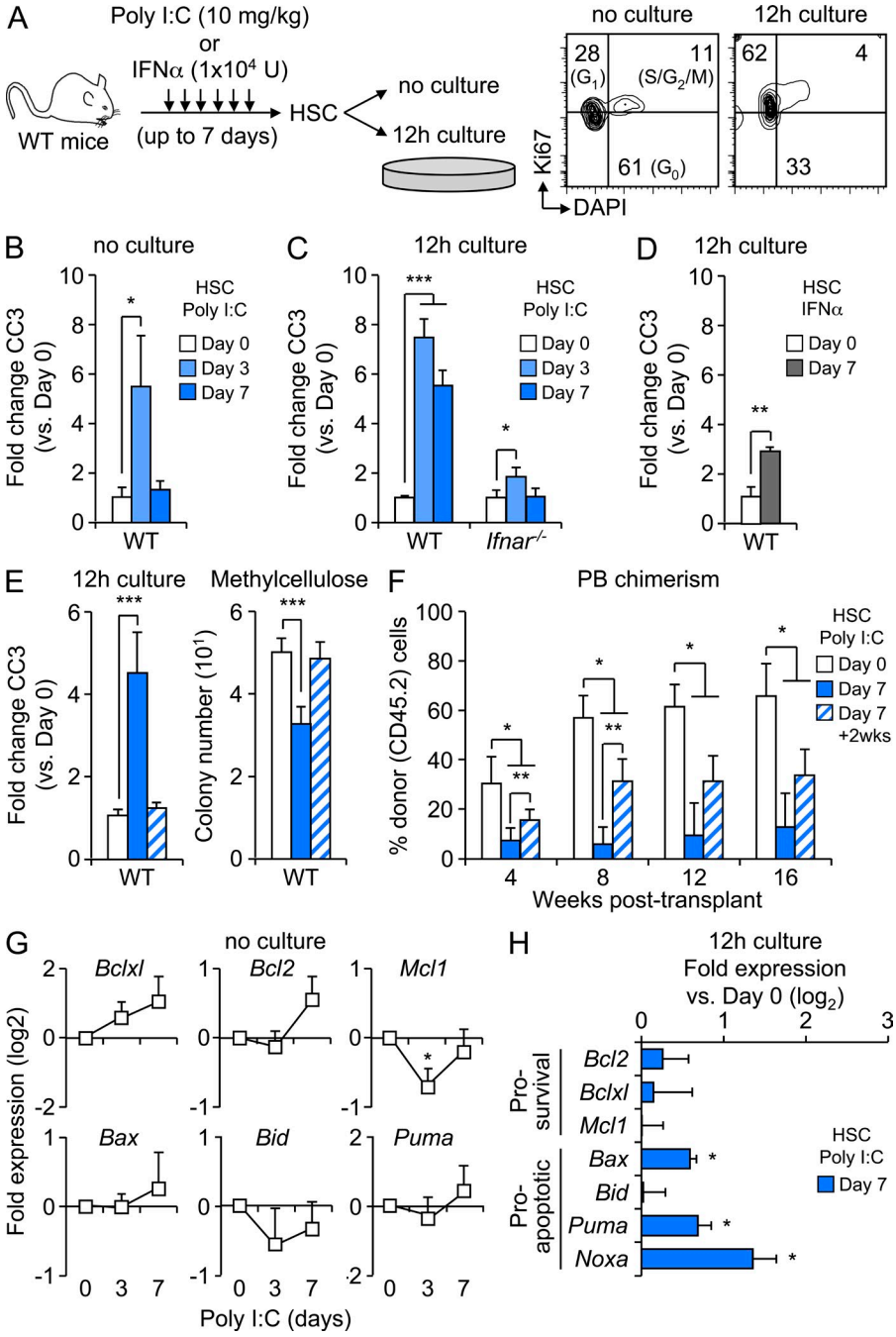

Figure 8. IFN-1s directly induce apoptosis in cycling HSCs. (A) Experimental design for apoptosis and gene expression analyses (left) and representative FACS plots for cell cycle distribution (right) in freshly isolated and 12-h cultured WT untreated HSCs. (B–D) CC3 levels in HSCs isolated from (B) poly I:C–treated WT mice without culture, (C) poly I:C–treated WT and *Ifnar*$^{-/-}$ mice after 12-h culture, and (D) IFN-α–treated WT mice after 12-h culture. Results are expressed as fold change relative to day 0 control HSCs in one representative experiment performed in triplicate. (E and F) Analyses of HSCs isolated from mice treated with poly I:C either for 0 and 7 d, or for 7 d followed by 2 wk recovery without poly I:C injections (7 + 2 wk) before harvest. (E) CC3 levels after 12-h culture (left) and mean numbers of colonies in 7-d methylcellulose culture (right). Results are expressed as fold change versus day 0 control HSCs in one representative experiment performed in triplicate. (F) PB chimerism over 16 wk after transplantation of 250 HSCs (isolated from pools of 3 mice/group) into lethally irradiated recipients (4–5 mice/group). (G) SABiosciences PCR array analyses for expression of *Bcl2* family genes in HSCs isolated from poly I:C–treated mice (n = 4, pools of 5 mice/group). Results are expressed as $\log_2$ fold expression relative to day 0 controls. (H) Quantitative RT-PCR analyses for *Bcl2* family gene expression in HSCs isolated from poly I:C–treated mice and cultured for 12 h (n = 3–4). Results are expressed as $\log_2$ fold expression relative to day 0 controls. All data are mean ± SD; statistical significance was determined by Student's t test (*, P ≤ 0.05; **, P ≤ 0.01; ***, P ≤ 0.005).

exposure induced HSC proliferation with similar kinetics in both control and *Trp53*$^{-/-}$ mice, and HSCs from *Trp53*$^{-/-}$ mice showed no significant delay in their return to quiescence compared with control HSCs (Fig. 9 F). Moreover, we observed similar results upon poly I:C treatment of *Foxo3a*$^{-/-}$ mice, which lack another important HSC quiescence-enforcer (Fig. 9 F). Collectively, these results demonstrate a key function of p53 in regulating the mitochondrial proapoptotic machinery in response to IFN-1 stimulation and indicate that no single transcription factor regulates the switch from quiescence to proliferation that briefly accompanied IFN-1 exposure in vivo, which instead relies on the concerted deactivation/reactivation of multiple quiescence-enforcing mechanisms (Fig. 9 G).

Enforced proliferation exacerbates IFN-1–mediated cell killing and depletes HSCs

Lastly, we investigated whether quiescence reentry during chronic IFN-1 treatment could protect IFN-exposed HSCs from the killing effect of myeloablative drugs and adapted the protocol previously used to demonstrate the impaired function of proliferating HSCs after acute IFN-1 exposure

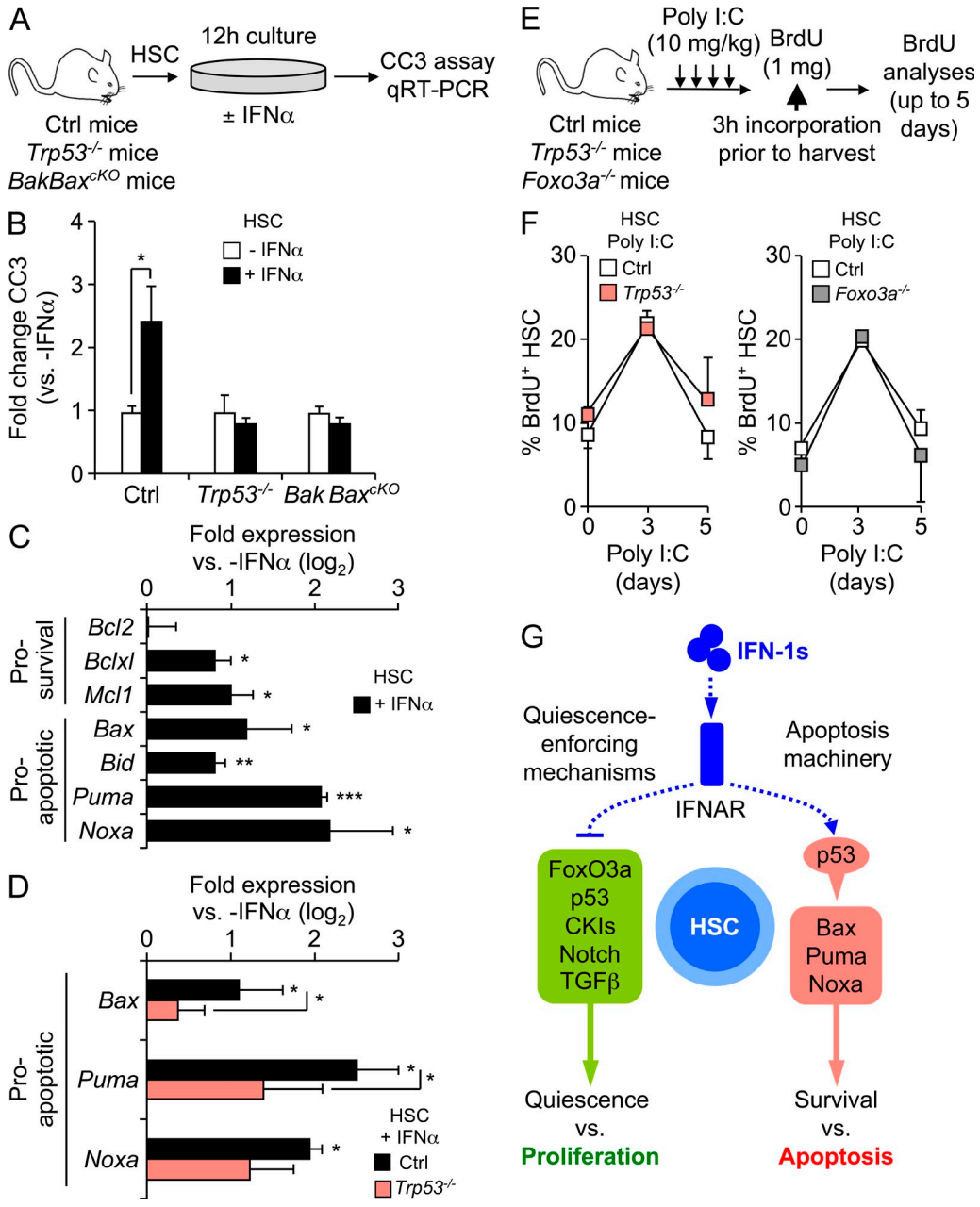

Figure 9. Role of p53 and intrinsic apoptosis pathway in IFN-1–exposed HSCs. (A) Experimental design for HSC apoptosis and gene expression assays. (B) CC3 levels in WT, *Trp53*$^{-/-}$, and *BakBax*^{cKO} HSCs treated for 12 h ± 100 ng/ml IFN-α (n = 3–4). Results are expressed as fold change relative to IFN-α control HSCs. (C and D) Quantitative RT-PCR analyses for *Bcl2* family gene expression in (C) WT and (D) Ctrl and *Trp53*$^{-/-}$ HSCs treated for 12 h ± 100 ng/ml IFN-α (n = 3–4). Results are expressed as $\log_2$ fold expression relative to IFN-α controls. (E) Experimental design for in vivo BrdU incorporation analyses in HSCs from poly I:C–treated Ctrl, *Trp53*$^{-/-}$, *Foxo3a*$^{-/-}$ mice. (F) Mean levels of BrdU incorporation in *Trp53*$^{-/-}$ (left) and *Foxo3a*$^{-/-}$ (right) mice compared with their respective Ctrl mice (3 mice/group). (G) Model for the role of p53 in IFN-1–exposed HSCs. All data are mean ± SD; statistical significance was determined by Student's t test (*, P ≤ 0.05; **, P ≤ 0.01; ***, P ≤ 0.005).

(Essers et al., 2009). Instead of injecting 5-fluorouracil (5-FU) at varying time points after acute (3-d) treatment with poly I:C, we injected mice treated with poly I:C for either 3 or 7 d with a single dose of 5-FU (150 mg/kg) directly after the poly I:C treatment period to study the impact of the initial cell cycle status of IFN-exposed HSCs on their survival and regeneration potential (Fig. 10 A). We also injected mice with 5-FU in the middle of a 7+7 d poly I:C treatment course to directly assess the effect of chronic IFN-1 exposure on HSC survival and regeneration potential (Fig. 10 A). As expected, we found significantly decreased survival in mice injected with 5-FU after acute IFN-induced HSC proliferation (day 3), compared with untreated mice (day 0) or mice with chronic IFN-exposed HSCs that had reentered quiescence (day 7;

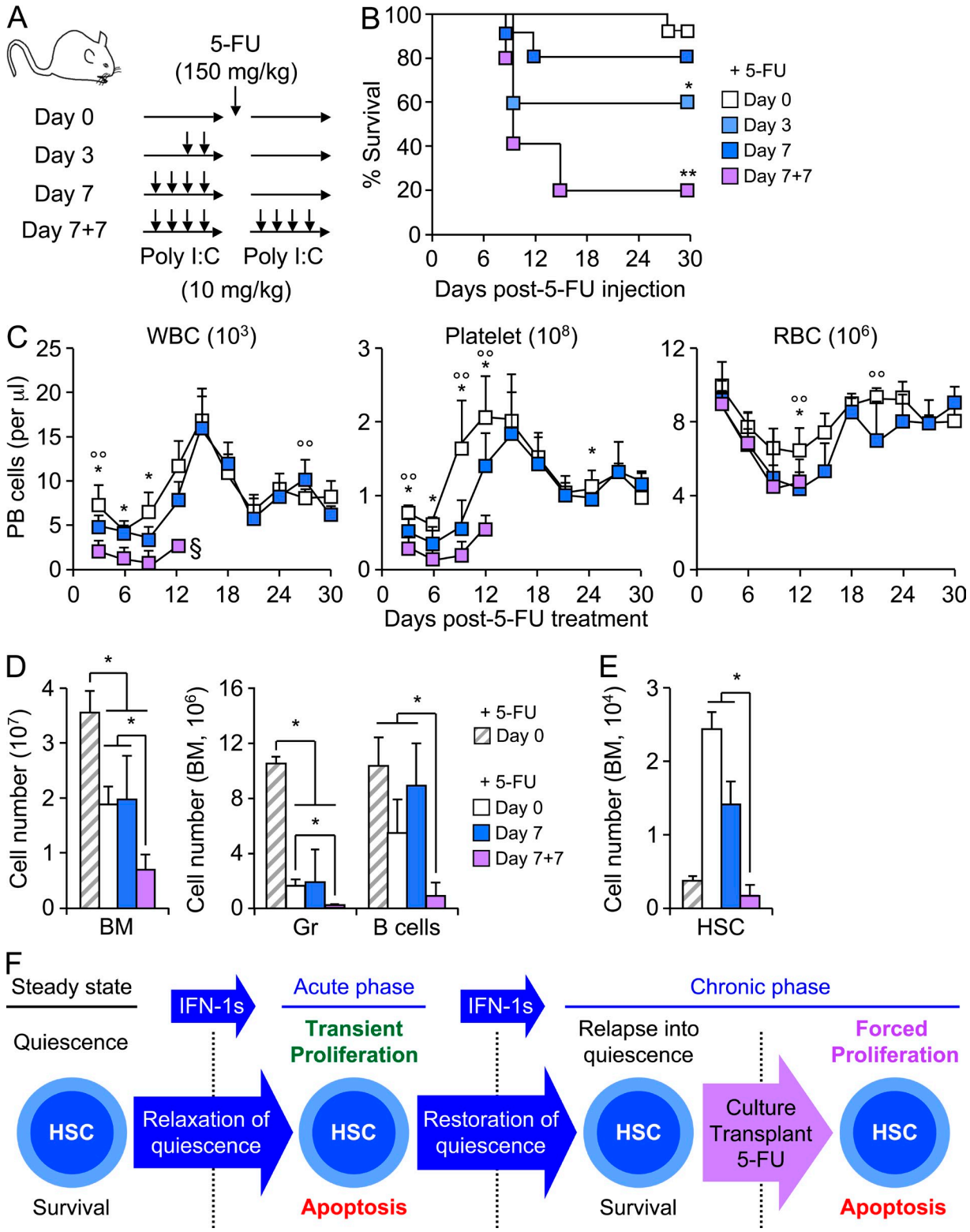

Figure 10. Enforced proliferation in the presence of IFN-1s depletes HSCs. (A) Experimental design. 5-FU injections were performed after 0, 3, or 7 d of poly I:C treatment, or in the middle of a 7 + 7 d cycle of poly I:C treatment. (B) Kaplan-Meyer survival curve for 5-FU–injected poly I:C–treated mice (5–10 mice/group). Statistical significance was determined by the Mantel-Cox test (*, $P \leq 0.05$). (C) Hematopoietic recovery in 5-FU–injected poly I:C–treated mice. Kinetics of white blood cell (WBC; left), platelet (Plt; middle), and RBC (right) recovery (5–10 mice/group). Data are mean ± SD; statistical significance was determined by Student's *t*-test (*, $P \leq 0.05$, day 0 vs. day 7 + 7; °°, $P \leq 0.05$, day 0 vs. day 7; §, insufficient number of mice remaining for

Fig. 10 B). Besides some delay in kinetics, we also observed recovery of all blood parameters in day 7 mice treated with 5-FU, indicating that IFN-exposed HSCs are still able to maintain blood production (Fig. 10 C). Strikingly, forcing IFN-exposed HSCs to proliferate in the constant presence of IFN-1s (day 7 + 7) resulted in a dramatic decrease in viability with 80% of the mice dead by 15 d after 5-FU injection (Fig. 10 B), and severely impaired blood recovery by 12 d after 5-FU injection (Fig. 10 C). Analyses performed at 10 d after 5-FU injection confirmed a substantial loss of BM cellularity in day 7 + 7 mice, with reduced Gr and B cell numbers compared with non–5-FU injected control mice and recovering day 0 and 7 mice (Fig. 10 D). We also quantified HSC numbers in these conditions using stringent HSC gating and the ESAM marker to confirm the absence of contaminating Sca-1–expressing progenitors (Fig. S4). Although recovering day 0 and 7 mice both showed increased HSC numbers, the HSC pool in day 7 + 7 mice was severely depleted to levels even lower than in non–5-FU injected control mice (Fig. 10 E). Collectively, these data indicate that whereas relapsing into quiescence protects IFN-1–exposed HSCs from apoptosis, forcing them to cycle in the constant presence of IFN-1s results in their depletion and subsequent inability to maintain blood homeostasis (Fig. 10 F).

DISCUSSION

In this study, we elucidate some of the complex effects of IFN-1s on HSC function. We show that HSC proliferation in vivo is a transient event despite chronic exposure to IFN-1s, which results from a brief down-regulation of a large number of quiescence-enforcing mechanisms that only occurs in vivo in the BM niche and not in vitro upon HSC culture. Importantly, we find that IFN-exposed HSCs quickly return to a quiescent state, where they remain largely protected from the apoptotic effects of IFN-1s unless forced to reenter the cell cycle after transplantation, culture, or regeneration from myeloablative treatments, at which point they activate a p53-dependent proapoptotic gene program. Altogether, our findings resolve numerous ambiguities related to the proliferative and suppressive effects of IFN-1s on HSC function. They identify the primary effect of chronic IFN-1s on HSCs as proapoptotic rather than proproliferative, and demonstrate that reentry into quiescence acts as a safeguard mechanism ensuring the survival of the HSC pool during chronic IFN-1 exposure.

Although the ability of acute IFN-1s to induce HSC proliferation is well known, as is the capacity of HSCs to return to quiescence after a single poly I:C injection (Essers et al., 2009), the effects of chronic IFN-1s on HSC cell cycle status have not been closely investigated. The observation that WT HSCs are selectively lost in WT:*Ifnar1*$^{-/-}$ BM chimeric mice upon poly I:C treatment supported the notion that chronic IFN-1 exposure could induce HSC proliferation and thereby their subsequent functional exhaustion (Essers et al., 2009). The idea that HSCs would proliferate continuously in the presence of IFNs is further supported by two studies directly investigating HSC proliferation 4 wk after either chronic *Mycobacterium avium* bacterial infection (which induces IFN-γ production) or continuous treatment with purified IFN-α, which both found elevated HSC cell cycle activity using BrdU incorporation and Ki67/Hoechst staining, respectively (Baldridge et al., 2010; Mullally et al., 2013). However, these studies only used a CD150^{+} LSK as phenotypic definition for HSCs that, as we show here, is not sufficient in the context of IFN exposure to exclude contamination by some actively cycling myeloid progenitors that have reacquired Sca-1 expression. In contrast, using the more stringent Flk2^{-}/CD48^{-}/CD150^{+} LSK phenotypic definition for HSCs and validation with the additional HSC marker ESAM, we find that after a short burst of acute proliferation, IFN-treated HSCs quickly reenter quiescence during chronic poly I:C treatment and then mostly remain dormant, despite continued IFN-1 exposure. Moreover, we show that the number of phenotypic HSCs remains constant through this period, suggesting that the depletion of WT HSCs in WT:*Ifnar1*$^{-/-}$ BM chimeric mice is likely the result of other IFN-1–mediated effects such as apoptosis, rather than continuous proliferation. Thus, our data support the idea that IFN-1–induced HSC proliferation is a transient event even in the presence of chronic IFN-1s, and is not sufficient to deplete the HSC pool.

The finding that IFN-1 induces acute HSC proliferation in vivo is paradoxical given that IFN-1 has long been described as an inhibitor of cell cycle activity in multiple cell types, including hematopoietic progenitors (Verma et al., 2002; Kiladjian et al., 2011). Indeed, we show that IFNs themselves are not intrinsically proproliferative, as neither IFN-α nor IFN-γ (de Bruin et al., 2013) are able to stimulate purified HSCs to proliferate in vitro, regardless of the concentration used. In addition, we found that IFN-α treatment directly blocks the cell cycle machinery in cultured HSCs, most likely by inducing expression of the CKIs *p27* and *p57*, and that coculture of HSCs with unfractionated BM cells or stromal cells does not reverse this direct antiproliferative effect of IFN-α exposure. These results suggest that IFNs do not directly trigger the cell cycle machinery beyond the level of activation

statistical analysis). (D and E) BM analysis of poly I:C–treated mice 10 d after 5-FU injection (4–5 mice/group). (D) BM cellularity (left) and Gr and B cells numbers (right). (E) HSC numbers. Data are mean ± SD; statistical significance was determined by Student's *t* test (*, P ≤ 0.05; **, P ≤ 0.01). (F) Model for how quiescence reentry protects HSCs from IFN-1–induced apoptosis. HSCs are normally maintained in a quiescent state buffered from proapoptotic stimuli. IFN-1s rapidly force HSCs into the cell cycle (acute IFN-1s) due to transient relaxation of quiescence-enforcing mechanisms, where they are vulnerable to apoptosis. During chronic IFN-1 exposure (chronic IFN-1s) HSCs return to a quiescent state where they remain largely protected from IFN-1–induced apoptosis unless forced back into the cell cycle, where they activate a p53-dependent proapoptotic gene program.

that already occurs in culture, and highlights the limitations of in vitro culture systems in accurately reproducing the physiological BM niche. They are also in sharp contrast with another published work showing increased BrdU incorporation in HSCs cultured with BM cells in the presence of IFN-γ for 12 h (Baldridge et al., 2010). However, these HSCs were identified after culture using the $CD150^+$ LSK phenotypic definition and, therefore, are likely contaminated by some actively cycling myeloid progenitors that have reacquired Sca-1 expression upon IFN-γ treatment. Collectively, these results indicate that the classical role of IFN-1s as anti-proliferative cytokines applies to HSCs, but only in vitro and not in an in vivo context.

So, why do IFN-1s induce transient HSC proliferation in vivo? Although we observe some of the previously reported changes in cell cycle genes in acutely proliferating IFN-1–exposed HSCs (i.e., increased *Ccne1* expression and decreased *Pten* levels; Essers et al., 2009), we also could not identify a broad gene signature reflecting direct activation of the proliferation machinery in vivo. Instead, we find decreased expression of many genes enforcing quiescence, including *Foxo3a*, *p53*, *p27*, *p57*, and components of the Notch and TGFβ pathways in acutely proliferating IFN-1–exposed HSCs in vivo. Consistently, we observe a complete recovery in the expression of quiescence-enforcing genes when HSCs reenter quiescence during chronic IFN-1 exposure. These changes likely reflect transient inactivation of quiescence-enforcing mechanisms to a threshold that allows a brief proliferation of the HSC pool. Moreover, our data suggest that this effect is based on inactivation of a broad set of mechanisms, as genetic deficiency in individual quiescence-enforcing transcription factors such as *Trp53* and *Foxo3a* are not sufficient to perturb the cell cycle behavior of IFN-1–exposed HSCs. As we do not observe decreased expression of IFNAR or IFN-1–regulated genes, the return of the HSC pool to quiescence likely reflects the activation of mechanisms known to restrain HSC proliferation in response to IFN-1s, such as *Irgm1*, *Irf2*, CD81, and/or TGFβ signaling (Sato et al., 2009; King et al., 2011; Lin et al., 2011; Brenet et al., 2013), rather than induction of an IFN-1–refractory state. Thus, our data support a model in which IFN-1s do not actively trigger the proliferative machinery of HSCs in vivo, but instead indirectly license HSCs to proliferate by transiently reducing the expression and activity of the complex regulatory network that enforces HSC quiescence in the BM niche. Such a model is supported by recent evidence that proliferating IFN-1–exposed HSCs alter their physical localization in the BM away from quiescence-enforcing periarteriolar niche cells (Kunisaki et al., 2013). It would also explain why the proliferative effect of IFN-1s is not observed in vitro, as most quiescence-enforcing mechanisms such as FoxO3a are already rapidly inactivated, regardless of the presence of IFN-1s, upon removal of HSCs from the BM niche and subsequent culture (Yamazaki et al., 2009).

IFN-1s have classically been described as death inducers, capable of triggering apoptosis via activation of a variety of mechanisms including proapoptotic *Bcl2* proteins such as *Bax*, and death ligands such as TRAIL and TNF (Kiladjian et al., 2011). Although HSC survival relies in large part on balanced expression of prosurvival and proapoptotic *Bcl2* genes, (Mohrin et al., 2010), a role for apoptosis in the effect of IFN-1s on HSC function has not been carefully investigated. Here, we find increased apoptosis in acutely proliferating IFN-treated HSCs, which likely results from decreased expression of the essential prosurvival factor *Mcl1* (Opferman et al., 2005) and tilts the balance of *Bcl2* family members toward cell death. However, once IFN-treated HSCs have reentered quiescence, they do not show detectable apoptosis levels unless they are subsequently forced to proliferate due to culture, transplantation or myeloablation treatment. In this context, IFN-1–exposed HSCs that reenter the cell cycle show a striking activation of a proapoptotic gene program with induction of *Bax*, *Noxa*, and *Puma*, which likely tilts the balance of *Bcl2* family members toward cell death. Our data therefore support a model in which IFN-1s poise HSCs for apoptosis but only trigger direct cell death in proliferating HSCs. This raises the intriguing possibility that the relapse of the HSC pool to a quiescent state after chronic IFN-1 treatment could result from the elimination of a subset of proliferating HSCs. Such a hypothesis would be consistent with models of an HSC hierarchy with dormant and active subpopulations (Wilson et al., 2008), but this would need to be directly tested. Our results are also consistent with the demonstration that IFN-1s can induce apoptosis via activation of cell cycle checkpoint mechanisms, including p53 and the IRF family of transcription factors (Takaoka, et al., 2003; Tamura et al., 2008). Indeed, *Bax*, *Puma*, and *Noxa* are well-known p53 target genes, and our data identify p53 as a key trigger mechanism for the induction of apoptosis in response to IFN-1 exposure. Because different splice isoforms of *Bcl2* family members can exhibit unique pro- or antiapoptotic activities (Goff et al., 2013), whether changes in splicing contribute to IFN-1–mediated apoptosis would also need to be investigated. Collectively, our results provide a mechanism for the proapoptotic effects of IFN-1 on HSCs, and an explanation for how chronic IFN-1 exposure can suppress blood production without exhausting the HSC compartment by demonstrating that reentry into quiescence acts as a safeguard mechanism ensuring the survival of the HSC pool during chronic IFN-1 exposure.

Our findings are relevant to human patients and may explain the relative rarity of BM failure syndromes caused by chronic IFN-1 production in the absence of other complicating factors (Zhou et al., 2007; Ioannou et al., 2010). In these conditions, the HSC compartment may remain quiescent and thus largely protected from the proapoptotic effects of IFN-1 exposure. Notably, patients suffering from an IFN-1–driven diseases, such as SLE, who undergo autologous BM transplantation experience a postprocedure mortality rate nearly 10-fold higher than other autoimmune patients (Tyndall, 2011; Szodoray et al., 2012). It would be interesting to assess whether the increase in transplant failure in SLE patients might be linked to decreased or delayed hematopoietic reconstitution, which in turn could be driven by an IFN-1–driven proapoptotic

program that is activated after mobilization and/or transplantation. Indeed, we directly illustrate the inherent fragility of quiescent IFN-exposed HSCs that are forced back into the cell cycle by showing decreased HSC engraftment after transplantation, as well as pronounced HSC depletion and poor survival upon 5-FU–mediated myeloablation in mice with chronic exposure to IFN-1s. Our results therefore support the idea that blockade of IFN-1s or their prodeath mechanisms may restore HSC potential in patients with chronic IFN-1, as a 2-wk recovery from IFN-1 exposure in mice returns HSC apoptosis and function to relatively normal levels. Interestingly, a recently published work shows that GATA3 activation via the p38 MAP kinase pathway also limits the long-term reconstitution capacity of IFN-1–exposed HSCs (Frelin et al., 2013). This suggests that IFN-1 may trigger a set of complementary mechanisms aimed at limiting the function of HSCs, which could be relevant in the context of viral infection. Collectively, these results suggest that blockade of IFN-1s or their downstream targets could substantially improve HSC function in individuals with chronic IFN-1s.

IFN administration has long been used therapeutically, albeit with mixed success, to treat a range of myeloproliferative neoplasms (MPN) originating from transformed HSCs with disease-propagating leukemic stem cell (LSC) activity, including CML- and $JAK2^{V617F}$-mediated essential thrombocytopenia (ET) and polycythemia vera (PV; Kiladjian et al., 2011). Our results may explain the limited efficacy of IFN-1 in inducing durable complete remission in CML patients because, during chronic IFN-1 exposure, the quiescent LSC compartment would remain largely insensitive to IFN-1–mediated apoptosis and would not be eliminated. Interestingly, treatment of mice with two sequential doses (up to 3 d) of poly I:C followed by 5-FU rendered proliferating IFN-exposed HSCs vulnerable to 5-FU–mediated killing (Essers et al., 2009), which raised the possibility that the in vivo proproliferative effects of IFN-1s could be used to sensitize quiescent LSCs to killing by tyrosine kinase inhibitors (TKI) such as Imatinib. These results provided a rationale for the success of combined Imatinib + IFN-1 therapy in curing some CML patients, and reignited interest in using IFNs to treat MPNs despite the severe toxicity associated with their use (Kiladjian et al., 2011). However, our findings would argue that the therapeutic window in which quiescent LSCs will be induced to proliferate by IFN-1s and thereby susceptible to TKI-mediated killing will be quite brief. Instead, they suggest that the poising of IFN-exposed LSCs toward apoptosis and their killing upon TKI treatment might be the mechanism underlying the therapeutic effects of IFN-1s, especially during the initial tumor debulking observed with TKI therapy. Interestingly, a recent work using a PV mouse model shows a preferential depletion of $Jak2^{V617F}$ LSCs compared with WT HSCs in WT:$Jak2^{V617F}$ BM chimeric mice after 4 wk treatment with IFN-α (Mullally et al., 2013). Although the authors propose that exaggerated cell cycle activity in $Jak2^{V617F}$ LSCs underlies this effect, it cannot be ruled out that it solely reflects contamination by cycling progenitors in the $CD150^+$ LSK gate used to define HSCs in this study, nor that differences in the IFN-mediated apoptosis response of normal versus transformed HSCs contribute to the specific elimination of $Jak2^{V617F}$ LSCs. Future studies will be needed to determine whether transformed HSCs are more sensitive to the killing effect of IFN-1 treatments, and to carefully define for each MPN disease-type the kinetics of LSC cell cycle activity and activation of apoptotic mechanisms during IFN-1 administration. Such understanding will be critical for optimizing their therapeutic effect on LSCs and minimizing their toxicity to nonleukemic cells, particularly when used in combination with other drugs such as TKIs.

Collectively, our results clarify the link between the proliferative and suppressive effects of IFN-1s on HSC function by showing that IFN-1s only transiently induce HSC proliferation in vivo, which seems to be an acute 'bystander' effect related to a brief relaxation of quiescence-enforcing mechanisms. This occurs alongside a broader proapoptotic effect consistent with the antiviral role of IFN-1s. Importantly, induction of a p53-dependent IFN-mediated proapoptotic gene program occurs exclusively in proliferating HSCs, which prevents wholesale exhaustion of the quiescent HSC pool, but also degrades the regenerative potential of HSCs and adversely affects the maintenance of blood homeostasis during chronic IFN-1 exposure. Our findings therefore elucidate how canonically antiproliferative, proapoptotic cytokines induce HSC proliferation and alter HSC function in a manner consistent with their role in chronic inflammation and autoimmune diseases.

MATERIALS AND METHODS

Mice. Congenic C57BL/6 WT mice were used as donors ($CD45.2^+$) and recipients ($CD45.1^+$) for all the experiments. *Ifnar1*$^{-/-}$, *Trp53*$^{-/-}$, *Foxo3a*$^{-/-}$, and *BakBax*^{cKO} mice have been described previously (Donehower et al., 1992; Müller et al., 1994; Castrillon et al., 2003; Warr et al., 2013). Transplantation of purified HSCs and generation of WT:*Ifnar1*$^{-/-}$ BM chimeric mice were performed as previously described (Santaguida et al., 2009). For poly I:C treatment, 6–12 wk-old age- and gender-matched mice were injected i.p. with 10 µg/g body mass of poly I:C (GE Healthcare) in PBS at 2-d intervals for up to 30 d. For in vivo IFN-α treatment, mice were injected subcutaneously with 1×10^4 U IFN-α4 (eBioscience) every 12 h until BM harvest. For in vivo HSC proliferation assays, mice were injected i.p. with 1 mg BrdU (Sigma-Aldrich) in D-PBS 3 h before BM harvest. For myeloablation treatment, mice were injected i.p. with 150 mg/kg of 5-FU (Sigma-Aldrich) in PBS, and PB was collected via the retro-orbital vein into K_2EDTA-coated collection tubes (BD) for complete blood counts (CBC) performed on a Hemavet950 analyzer (DREW Scientific). All mouse experiments were performed in accordance with the Institutional Animal Care and Use Committee at the University of California, San Francisco.

Flow cytometry. Hematopoietic stem and progenitor cell surface staining and enrichment procedures were done as described previously (Santaguida et al., 2009). Cells were isolated on a FACS ARIAII (BD) using double sorting for maximum purity, and analyzed on a FACS LSRII (Becton Dickinson). Cellularity was determined on one tibia and one femur per mouse using a ViCell automated cell counter (Beckman-Coulter). Surface staining for IFNAR1 was performed with a PE-conjugated antibody (BD). BrdU staining and analysis of PB for CD45.1/CD45.2 chimerism were performed as

previously described (Santaguida et al., 2009). For intracellular Ki67/DAPI staining, BM cells were stained with surface markers, fixed, and permeabilized using a Cytofix/Cytoperm kit according to the manufacturer's instructions (BD) and stained with an anti–Ki67-FITC antibody (Vector Laboratories) for 1 h at room temperature. DAPI was added to cell samples and allowed to incubate for 20 min at RT before analysis. Intracellular phospho-AKT was performed as previously described (Chen et al., 2009).

Immunofluorescence analyses. For FoxO3a detection, HSCs (1,000/slide) were sorted directly onto PolyPrep L-lysine-coated slides (Sigma-Aldrich), fixed with 4% paraformaldehyde, blocked with 0.1% BSA in PBS, permeabilized with 0.2% Triton X-100, stained for 1 h at room temperature with an anti-FoxO3a antibody (Millipore), incubated for 1 h at room temperature with a goat anti–rat A549 antibody (Invitrogen), and mounted with coverslips in VectaShield (Vector Laboratories) containing 1 ng/ml DAPI. For EdU assays, HSCs (1,500/slide) were sorted onto slides and fixed in 4% PFA as described above, and EdU incorporation was detected using A594-labeled azide click chemistry according to the manufacturer's instructions (Life Technologies). For cleaved caspase 3 (CC3) detection in BM sections, femurs were snap-frozen in OCT, and 10-µm sections were made on a CM1850 Cryostat using the CryoJane tape transfer system (Leica). Slides were subsequently air-dried for 3 h, fixed in 4% PFA, blocked in 0.1% Triton X-100 containing 10% goat serum, stained overnight at 4°C with an anti-CC3 antibody (Cell Signaling Technology), incubated for 1 h at room temperature with a donkey anti–rabbit A488 antibody (Invitrogen), stained with 1 ng/ml DAPI, and mounted with coverslips. Immunofluorescence images were acquired on a TCS-SP5 microscope (Leica) and analyzed using Velocity software (Perkin-Elmer). For EdU incorporation assays, at least 200 cells were scored per replicate slide.

Cell culture. For colony assays, HSCs (100/dish) were grown for 7 d in MethoCult M3231 methylcellulose media (StemCell Technologies) supplemented with SCF (10 ng/ml), IL-11 (10 ng/ml), Flt3L (10 ng/ml), IL-3 (10 ng/ml), GM-CSF (10 ng/ml), TPO (100 ng/ml), and EPO (10^4 U/ml; all from PeproTech). For growth in liquid culture, HSCs (400/well) were cultured in StemPro34 medium (Invitrogen) supplemented with SCF, Flt3L, and TPO. For expansion analyses, cells were manually counted with a hemocytometer after 8 d. For apoptosis detection, Caspase-Glo (Promega) luminescent reagent was added at a 1:1 ratio after 12 h of culture and incubated according to the manufacturer's instructions. Luminescence was read using a plate-based luminometer (BioTek). For in vitro BrdU incorporation, HSCs (2,500/well) were cultured for 12 h in StemPro34 medium supplemented with SCF, TPO, and 60 µM BrdU. For BM co-culture experiments, CFSE-labeled HSCs (2,500/well) were incubated with unfractionated BM cells (5×10^5) for up to 48 h in StemPro34 medium supplemented with SCF and TPO. For OP9-DL1 co-culture experiments, CellTracker Violet-labeled HSCs (2,500/well) were added atop OP9-DL1 stromal cells (5×10^3/well) in IMDM supplemented with 5% FBS, SCF, TPO, TGF-β (10 ng/ml; PeproTech) and 10 µM EdU as described (Santaguida et al., 2009). For CFSE labeling, HSCs were incubated for 10 min with 5 µM CFSE (Molecular Probes) in PBS, quenched with FBS, and washed twice before culture. Mouse recombinant IFN-α4 (eBioscience) was added to the culture at 100 ng/ml except when indicated.

Gene expression analyses. For SA Biosciences PCR arrays, total RNA was isolated from 20,000 HSCs sorted directly into TRIzol-LS (Invitrogen) using the Arcturus PicoPure RNA kit and genomic DNA was removed using the QIAGEN RNase-free DNase kit following manufacturer's protocols. Purified RNA was quantified on a Bioanalyzer (Agilent) and 4 ng were subjected to RT and 12 rounds of preamplification using the RT² Reverse transcription kit and target-specific primers for custom-designed RT² Profiler qRT-PCR arrays (SA Biosciences). Array plates were run on an Applied Biosystems HT7900 thermocycler and analyzed using the ΔC_T method. For standard quantitative RT-PCR, total RNA extraction and qRT-PCR analyses were performed as previously described (Mohrin et al., 2010).

Cytokine analysis. Blood was harvested after euthanasia via cardiac puncture and serum was analyzed for cytokines using a Luminex xMAP 20-plex mouse cytokine array according to the manufacturer's instructions. ELISA analyses of serum TNF, MCP-1, and IFN-α were performed according to the manufacturer's instructions (eBioscience).

Statistics. Measurements were performed in triplicate and *n* indicated the number of independent experiments. Data were expressed as mean ± SD. Statistical significance was determined using a two-tailed, unpaired Student's *t* test. Significance of survival data were determined using a log-rank (Mantel-Cox) test. P-values of ≤0.05 were considered statistically significant.

Online supplemental material. Fig. S1 shows FACS gating strategy for analysis of mature and immature BM populations. Fig. S2 shows FACS gating scheme for analysis of BrdU staining, Ki67/DAPI staining, and phospho-AKT levels in HSCs. Fig. S3 shows FACS gating for identification and recovery of labeled HSCs in BM and OP9-DL1 co-culture experiments. Fig. S4 shows FACS gating scheme for analysis of HSCs in poly I:C– and 5-FU–injected mice. Online supplemental material is available at http://www.jem.org/cgi/content/full/jem.20131043/DC1.

We thank Dr. Jason Cyster for critical reading of this manuscript, Michael Kissner for management of the Broad Center Flow Cytometry Core Facility, and all members of the Passegué laboratory for helpful comments and discussions.

E.M.P. was supported by postdoctoral Ruth L. Kirschstein National Research Service Awards (NRSA) T32 CA108462, T32 AI007334 and F32 HL106989. R.L. was supported by a CIRM Bridges Fellowship. This work was supported by R01 HL092471 and CIRM New Faculty Award RN2-00934 to E.P.

The authors declare no financial conflicts of interest.

Submitted: 20 May 2013
Accepted: 13 January 2014

REFERENCES

Bakker, S.T., and E. Passegué. 2013. Resilient and resourceful: genome maintenance strategies in hematopoietic stem cells. *Exp. Hematol.* 41:915–923 (Epub ahead of print). http://dx.doi.org/10.1016/j.exphem.2013.09.007

Baldridge, M.T., K.Y. King, N.C. Boles, D.C. Weksberg, and M.A. Goodell. 2010. Quiescent haematopoietic stem cells are activated by IFN-gamma in response to chronic infection. *Nature*. 465:793–797. http://dx.doi.org/10.1038/nature09135

Brenet, F., P. Kermani, R. Spektor, S. Rafii, and J.M. Scandura. 2013. TGFβ restores hematopoietic homeostasis after myelosuppressive chemotherapy. *J. Exp. Med*. 210:623–639. http://dx.doi.org/10.1084/jem.20121610

Castrillon, D.H., L. Miao, R. Kollipara, J.W. Horner, and R.A. DePinho. 2003. Suppression of ovarian follicle activation in mice by the transcription factor Foxo3a. *Science*. 301:215–218. http://dx.doi.org/10.1126/science.1086336

Chen, C., Y. Liu, Y. Liu, and P. Zheng. 2009. mTOR regulation and therapeutic rejuvenation of aging hematopoietic stem cells. *Sci. Signal*. 2:ra75.

Davis, L.S., J. Hutcheson, and C. Mohan. 2011. The role of cytokines in the pathogenesis and treatment of systemic lupus erythematosus. *J. Interferon Cytokine Res.* 31:781–789. http://dx.doi.org/10.1089/jir.2011.0047

de Bruin, A.M., O. Demirel, B. Hooibrink, C.H. Brandts, and M.A. Nolte. 2013. Interferon-γ impairs proliferation of hematopoietic stem cells in mice. *Blood*. 121:3578–3585. http://dx.doi.org/10.1182/blood-2012-05-432906

Donehower, L.A., M. Harvey, B.L. Slagle, M.J. McArthur, C.A. Montgomery Jr., J.S. Butel, and A. Bradley. 1992. Mice deficient for p53 are developmentally normal but susceptible to spontaneous tumours. *Nature*. 356:215–221. http://dx.doi.org/10.1038/356215a0

Dumont, F.J., and L.Z. Coker. 1986. Interferon-α/β enhances the expression of Ly-6 antigens on T cells in vivo and in vitro. *Eur. J. Immunol*. 16:735–740. http://dx.doi.org/10.1002/eji.1830160704

Essers, M.A., S. Offner, W.E. Blanco-Bose, Z. Waibler, U. Kalinke, M.A. Duchosal, and A. Trumpp. 2009. IFNalpha activates dormant haematopoietic

stem cells in vivo. *Nature*. 458:904–908. http://dx.doi.org/10.1038/nature07815

Feng, C.G., D.C. Weksberg, G.A. Taylor, A. Sher, and M.A. Goodell. 2008. The p47 GTPase Lrg-47 (Irgm1) links host defense and hematopoietic stem cell proliferation. *Cell Stem Cell*. 2:83–89. http://dx.doi.org/10.1016/j.stem.2007.10.007

Frelin, C., R. Herrington, S. Janmohamed, M. Barbara, G. Tran, C.J. Paige, P. Benveniste, J.C. Zuñiga-Pflücker, A. Souabni, M. Busslinger, and N.N. Iscove. 2013. GATA-3 regulates the self-renewal of long-term hematopoietic stem cells. *Nat. Immunol.* 14:1037–1044. http://dx.doi.org/10.1038/ni.2692

Goff, D.J., A.C. Recart, A. Sadarangani, H.J. Chun, C.L. Barrett, M. Krajewska, H. Leu, J. Low-Marchelli, W. Ma, A.Y. Shih, et al. 2013. A Pan-BCL2 inhibitor renders bone-marrow-resident human leukemia stem cells sensitive to tyrosine kinase inhibition. *Cell Stem Cell*. 12:316–328. http://dx.doi.org/10.1016/j.stem.2012.12.011

Gokce, M., Y. Bilginer, N. Besbas, F. Ozaltin, M. Cetin, F. Gumruk, and S. Ozen. 2012. Hematological features of pediatric systemic lupus erythematosus: suggesting management strategies in children. *Lupus*. 21:878–884. http://dx.doi.org/10.1177/0961203312443721

Hartner, J.C., C.R. Walkley, J. Lu, and S.H. Orkin. 2009. ADAR1 is essential for the maintenance of hematopoiesis and suppression of interferon signaling. *Nat. Immunol.* 10:109–115. http://dx.doi.org/10.1038/ni.1680

Ioannou, S., G. Hatzis, I. Vlahadami, and M. Voulgarelis. 2010. Aplastic anemia associated with interferon alpha 2a in a patient with chronic hepatitis C virus infection: a case report. *J. Med. Case Reports*. 4:268. http://dx.doi.org/10.1186/1752-1947-4-268

Kiladjian, J.J., R.A. Mesa, and R. Hoffman. 2011. The renaissance of interferon therapy for the treatment of myeloid malignancies. *Blood*. 117:4706–4715. http://dx.doi.org/10.1182/blood-2010-08-258772

King, K.Y., M.T. Baldridge, D.C. Weksberg, S.M. Chambers, G.L. Lukov, S. Wu, N.C. Boles, S.Y. Jung, J. Qin, D. Liu, et al. 2011. Irgm1 protects hematopoietic stem cells by negative regulation of IFN signaling. *Blood*. 118:1525–1533. http://dx.doi.org/10.1182/blood-2011-01-328682

Kunisaki, Y., I. Bruns, C. Scheiermann, J. Ahmed, S. Pinho, D. Zhang, T. Mizoguchi, Q. Wei, D. Lucas, K. Ito, et al. 2013. Arteriolar niches maintain haematopoietic stem cell quiescence. *Nature*. 502:637–643. http://dx.doi.org/10.1038/nature12612

Lin, K.K., L. Rossi, N.C. Boles, B.E. Hall, T.C. George, and M.A. Goodell. 2011. CD81 is essential for the re-entry of hematopoietic stem cells to quiescence following stress-induced proliferation via deactivation of the Akt pathway. *PLoS Biol*. 9:e1001148. http://dx.doi.org/10.1371/journal.pbio.1001148

Mohrin, M., E. Bourke, D. Alexander, M.R. Warr, K. Barry-Holson, M.M. Le Beau, C.G. Morrison, and E. Passegué. 2010. Hematopoietic stem cell quiescence promotes error-prone DNA repair and mutagenesis. *Cell Stem Cell*. 7:174–185. http://dx.doi.org/10.1016/j.stem.2010.06.014

Mullally, A., C. Bruedigam, L. Poveromo, F.H. Heidel, A. Purdon, T. Vu, R. Austin, D. Heckl, L.J. Breyfogle, C.P. Kuhn, et al. 2013. Depletion of Jak2V617F myeloproliferative neoplasm-propagating stem cells by interferon-α in a murine model of polycythemia vera. *Blood*. 121:3692–3702. http://dx.doi.org/10.1182/blood-2012-05-432989

Müller, U., U. Steinhoff, L.F. Reis, S. Hemmi, J. Pavlovic, R.M. Zinkernagel, and M. Aguet. 1994. Functional role of type I and type II interferons in antiviral defense. *Science*. 264:1918–1921. http://dx.doi.org/10.1126/science.8009221

Ooi, A.G., H. Karsunky, R. Majeti, S. Butz, D. Vestweber, T. Ishida, T. Quertermous, I.L. Weissman, and E.C. Forsberg. 2009. The adhesion molecule esam1 is a novel hematopoietic stem cell marker. *Stem Cells*. 27:653-661.

Opferman, J.T., H. Iwasaki, C.C. Ong, H. Suh, S. Mizuno, K. Akashi, and S.J. Korsmeyer. 2005. Obligate role of anti-apoptotic MCL-1 in the survival of hematopoietic stem cells. *Science*. 307:1101–1104. http://dx.doi.org/10.1126/science.1106114

Orford, K.W., and D.T. Scadden. 2008. Deconstructing stem cell self-renewal: genetic insights into cell-cycle regulation. *Nat. Rev. Genet*. 9:115–128. http://dx.doi.org/10.1038/nrg2269

Passegué, E., and P. Ernst. 2009. IFN-alpha wakes up sleeping hematopoietic stem cells. *Nat. Med*. 15:612–613. http://dx.doi.org/10.1038/nm0609-612

Pietras, E.M., M.R. Warr, and E. Passegué. 2011. Cell cycle regulation in hematopoietic stem cells. *J. Cell Biol*. 195:709–720. http://dx.doi.org/10.1083/jcb.201102131

Platanias, L.C. 2005. Mechanisms of type-I- and type-II-interferon-mediated signalling. *Nat. Rev. Immunol*. 5:375–386. http://dx.doi.org/10.1038/nri1604

Santaguida, M., K. Schepers, B. King, A.J. Sabnis, E.C. Forsberg, J.L. Attema, B.S. Braun, and E. Passegué. 2009. JunB protects against myeloid malignancies by limiting hematopoietic stem cell proliferation and differentiation without affecting self-renewal. *Cancer Cell*. 15:341–352. http://dx.doi.org/10.1016/j.ccr.2009.02.016

Sato, T., N. Onai, H. Yoshihara, F. Arai, T. Suda, and T. Ohteki. 2009. Interferon regulatory factor-2 protects quiescent hematopoietic stem cells from type I interferon-dependent exhaustion. *Nat. Med*. 15:696–700. http://dx.doi.org/10.1038/nm.1973

Szodoray, P., L. Varoczy, G. Papp, S. Barath, B. Nakken, G. Szegedi, and M. Zeher. 2012. Immunological reconstitution after autologous stem cell transplantation in patients with refractory systemic autoimmune diseases. *Scand. J. Rheumatol*. 41:110–115. http://dx.doi.org/10.3109/03009742.2011.606788

Takaoka, A., S. Hayakawa, H. Yanai, D. Stoiber, H. Negishi, H. Kikuchi, S. Sasaki, K. Imai, T. Shibue, K. Honda, and T. Taniguchi. 2003. Integration of interferon-αβ signalling to p53 resonses in tumour suppression and antiviral defence. *Nature*. 424:517–523.

Talpaz, M., H. Kantarjian, R. Kurzrock, J.M. Trujillo, and J.U. Gutterman. 1991. Interferon-alpha produces sustained cytogenetic responses in chronic myelogenous leukemia. Philadelphia chromosome-positive patients. *Ann. Intern. Med*. 114:532–538. http://dx.doi.org/10.7326/0003-4819-114-7-532

Tamura, T., H. Yanai, D. Savitsky, and T. Taniguchi. 2008. The IRF family transcription factors in immunity and oncogenesis. *Annu. Rev. Immunol*. 26:535–584. http://dx.doi.org/10.1146/annurev.immunol.26.021607.090400

Tyndall, A. 2011. Successes and failures of stem cell transplantation in autoimmune diseases. *Hematology (Am Soc Hematol Educ Program)*. 2011:280–284. http://dx.doi.org/10.1182/asheducation-2011.1.280

Verma, A., D.K. Deb, A. Sassano, S. Uddin, J. Varga, A. Wickrema, and L.C. Platanias. 2002. Activation of the p38 mitogen-activated protein kinase mediates the suppressive effects of type I interferons and transforming growth factor-β on normal hematopoiesis. *J. Biol. Chem*. 277:7726–7735. http://dx.doi.org/10.1074/jbc.M106640200

Warr, M.R., M. Binnewies, J. Flach, D. Reynaud, T. Garg, R. Malhotra, J. Debnath, and E. Passegué. 2013. FOXO3A directs a protective autophagy program in haematopoietic stem cells. *Nature*. 494:323–327. http://dx.doi.org/10.1038/nature11895

Wilson, A., E. Laurenti, G. Oser, R.C. van der Wath, W. Blanco-Bose, M. Jaworski, S. Offner, C.F. Dunant, L. Eshkind, E. Bockamp, et al. 2008. Hematopoietic stem cells reversibly switch from dormancy to self-renewal during homeostasis and repair. *Cell*. 135:1118–1129. http://dx.doi.org/10.1016/j.cell.2008.10.048

Yamazaki, S., A. Iwama, S.-I. Takayanagi, Y. Morita, K. Eto, H. Ema, and H. Nakauchi. 2006. Cytokine signals modulated via lipid rafts mimic niche signals and induce hibernation in hematopoietic stem cells. *EMBO J.* 25:3515–3523. http://dx.doi.org/10.1038/sj.emboj.7601236

Yamazaki, S., A. Iwama, S. Takayanagi, K. Eto, H. Ema, and H. Nakauchi. 2009. TGF-beta as a candidate bone marrow niche signal to induce hematopoietic stem cell hibernation. *Blood*. 113:1250-1256.

Zhao, X., G. Ren, L. Liang, P. Ai, B. Zheng, J. Tischfield, Y. Shi, and C. Shao. 2009. Brief Report-IFNgamma Induces Expansion of Lin-Sca-1+ C-Kit+ Cells. *Stem Cells*. 28:122–126.

Zhou, L., J. Opalinska, and A. Verma. 2007. p38 MAP kinase regulates stem cell apoptosis in human hematopoietic failure. *Cell Cycle*. 6:534–537. http://dx.doi.org/10.4161/cc.6.5.3921